ELSEVIER

Biophysical Chemistry 54 (1995) 1–33

Biophysical Chemistry

Structure and function of a molecular machine: cytochrome *c* oxidase

Francesco Malatesta [a,*], Giovanni Antonini [a], Paolo Sarti [b], Maurizio Brunori [c]

[a] *Department of Experimental Medicine, University of Rome 'Tor Vergata', Rome, Italy*
[b] *Institute of Biological Chemistry, University of Cagliari, Cagliari, Italy*
[c] *Department of Biochemical Sciences and CNR Center for Molecular Biology, University of Rome 'La Sapienza', Rome, Italy*

Received 17 November 1993; revised 17 May 1994; accepted 5 September 1994

Abstract

Cytochrome *c* is responsible for over 90% of the dioxygen consumption in the living cell and contributes to the build-up of a proton electrochemical gradient derived by the vectorial transfer of electrons between cytochrome *c* and molecular oxygen. The metal ions found in cytochrome oxidases play a crucial role in these processes and have been extensively studied. In this review we present and discuss some of the relevant spectroscopic and kinetic properties of the prosthetic groups of cytochrome *c* oxidase.

Keywords: Metalloproteins; Cytochrome *c* oxidase; Electron transfer; Membrane proteins; Energy transduction

Abbreviations: COX: cytochrome *c* oxidase (E.C. 1.9.3.1); COV: cytochrome oxidase vesicles; eT: electron transfer; EPR: electron paramagnetic resonance; MCD: magnetic circular dichroism; RR: resonance Raman; RCR: respiratory control ratio; SVD: singular value decomposition

* Corresponding author. Present address: Department of Biochemical Sciences 'A. Rossi Fanelli', University of Rome 'La Sapienza', P.le A. Moro 5, 00185 Rome, Italy.

SSDI 0301-4622(94)00117-0

1. Structure of cytochrome *c* oxidase

1.1. Introduction

Cytochrome *c* oxidase (ferrocytochrome *c*: O_2 oxidoreductase, EC 1.9.3.1) is an oligomeric metalloprotein incorporated in the mitochondrial inner membrane of eukaryotic cells or in the plasma membrane of bacteria [1–3]. This enzyme catalyses the transfer of electrons between two substrates, namely ferrocytochrome *c* and molecular oxygen, protons being consumed during the reaction. Part of the free energy of the reaction (the redox gap between cytochrome *c* and molecular oxygen is *ca.* 0.5 V at 25°C) is used to drive translocation of protons from the aqueous matrix to the intermembrane space of mitochondria [4] against an electrochemical gradient. Thus, cytochrome *c* oxidase is a redox-linked proton pump, which couples redox energy to the endoergonic vectorial transport of protons, in line with the chemiosmotic theory [5].

According to a classical viewpoint, electron transfer and energy transduction by cytochrome *c* oxidase are achieved by at least two different transition metals (copper and iron), organized in three distinct centers. By functional criteria these may be classified [1] on the basis of the substrate with which they interact directly. Two centers are the sites of electron donation by the macromolecular substrate cytochrome *c*, which is located in the mitochondrial intermembrane space. These are: (a) one heme *a* Fe, bearing a formyl group and a long isoprenoid side chain, called cytochrome *a* and (b) an EPR-detectable copper ion called Cu_A or Cu_a, since it is a partner of cytochrome *a* and follows its kinetic behavior. The other cluster, the prosthetic group which binds and reduces dioxygen to water, is a heterobinuclear center contributed by one iron and one copper ion in close proximity. The iron atom is inserted into an otherwise identical heme *a* which, however, is located in a protein environment which confers to this heme *a* quite distinct properties from cytochrome *a*; it is referred to as the cytochrome a_3 site and is within 5 Å from a copper ion, called Cu_B or Cu_{a3}, which under ordinary conditions is not detectable by EPR.

In this paper, current concepts on the structure, the metal centers and the kinetic properties of the enzyme and its proton pumping function will be reviewed in order to support the reader with critical discussions of possible mechanisms of electron transfer and energy transduction. Open questions relative to any of the above topics will also be highlighted, since some generally accepted dogmas, such as metal composition, have been recently challenged.

1.2. Structure and membrane topology

The number and type of subunits involved in the assembly of a fully competent cytochrome oxidase, the oligomeric state of the enzyme in situ (whether monomeric or dimeric), and the relationships of the enzyme with the membrane, have been actively investigated. Uncertainty originates from lack of both the tridimensional structure and knowledge of specific function(s) of all copurified subunits. Here we summarize some general features of mammalian cytochrome *c* oxidase, with some reference to bacterial oxidases.

Mammalian cytochrome oxidase is integral to the inner mitochondrial membrane. With few exceptions, the enzyme purified from beef heart following by and large Yonetani's procedure [6,7] is in a dimeric state [8–10]; monomeric oxidase has been purified from shark [11] or to some extent from camel heart [12].

Several authors have argued that the dimeric assembly is essential for redox activity, i.e. that the reaction catalysed by COX [see Section 2.1, Eq. (1)], is carried out by a dimeric oxidase [13]. This hypothesis was based partly on the fact that covalent binding of one cytochrome *c* per dimer leads to complete inactivation of the enzyme (the so-called half-of-sites effect) [14]. A different viewpoint has been advocated by Wilson and coworkers [11,12] on the basis of their results on cytochrome oxidase purified from shark heart (*Sphyrna lewini*), which was found to be fully active in spite of being monomeric; the assessment of the aggregation state of shark COX has been confirmed by equilibrium ultracentrifugation [15]. Monomeric COX may also be obtained from bovine enzyme following removal of subunit III ([16] and see [17] for a review) which allows to position subunit III at the interface in the dimer. The kinetics of oxidation of cytochrome *c* by III-less COX are very much similar to the native protein in detergent solution; in vesicles, however, the efficiency of proton translocation is reduced. In conclusion, monomeric COX is fully competent in carrying out the redox chemistry and also redox-linked proton translocation (Section 3) has been demonstrated; thus the dimeric state of COX isolated from mammalian sources is apparently not essential for its function in vitro. An important issue is to establish the aggregation state of COX in vivo. A rather simple way to distinguish monomeric from dimeric COX has been provided from CO displacement experiments at low protein concentration (to attenuate intermolecular interactions) [18,19]. We have used this approach to examine the aggregation state of COX reconstituted into phospholipid vesicles with the finding that monomeric COX (bovine III-less) behaves as a dimer or functionally interacting monomers when inserted into vesicle membrane. This view is not completely shared [10], therefore the issue is still open and further experiments are required.

Each monomer is formed by 13 subunits (polypeptides), associated in a 1 to 1 stoichiometry [20,21], with the exception of subunit VIIIb present in two copies. Subunits I, II, and III are the largest, and are present in all oxidases with a few exceptions, like the 2-subunit enzymes purified from *Thermus thermophilus* or from *Sulfolobus acidocaldarius* [22,23]; sometimes subunit III, more hydrophobic and loosely bound, is lost during enzyme purification. The major subunits are coded for by mitochondrial DNA, and the relative polypeptides are synthesized in the mitochondrial matrix. The remaining subunits are smaller, nuclear-coded, synthesized in the cytosol, and most often missing in the prokaryotic enzymes [24].

As an integral membrane protein, the mitochondrial enzyme spans the membrane completely. It conforms to the basic paradigm of being so structured to allow proper hydrophobic interactions with the non-polar components of the phospholipid bilayer. Thus 8 polypeptides out of 12 contain sequences of apolar aminoacids long enough (about 20 residues) to span the membrane in an alfa-helical conformation [1]. On the basis of EM image-reconstruction carried out originally on two-dimensional crystals a monomeric unit has been grossly depicted as Y-shaped, with the two arms inserted into the bilayer and the stem of Y protruding in the external bulk phase [25–27]. More recent cryo-EM observations [28], carried out on mitochondrial vesicles crystals containing ice-embedded molecules of cytochrome oxidase, provided the best up-date reconstruction of the dimeric membrane–protein unit. Fig. 1 reports the model of the dimer and its topology with reference to the bilayer. The results are consistent with the Y-shape originally proposed, but with some important differences: (a) approximately 70% of the total mass of the dimer, 110 Å long, appears to extend in the cytosolic phase, and contains a central cavity now proposed as the binding cleft for cytochrome *c* [28]; (b) in contrast with previous observations carried out with negatively stained

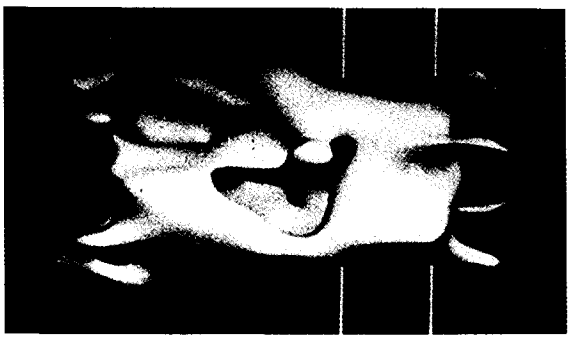

Fig. 1. Cytochrome oxidase structure and membrane topology. Modified from [28] with permission.

specimens [29], the hydrophobic region of the protein appears as a single compact domain, and separation of two distinct domains is clearly visible only out of the membrane plane, towards the matrix [28]. The degree of image resolution is certainly improved though the predicted transmembrane helices cannot be accommodated in the apparent volume of the membrane domain [28].

1.3. Metals

As discussed by Steffens et al. [30], the metal composition of COX has been quite controversial since the discovery of this enzyme by Warburg [31]. If general consensus is found for two heme irons (cytochrome *a* and cytochrome a_3) per functional unit of the enzyme (which may be defined as that containing 13 polypeptides with an overall molecular mass of ca. 200 kDa), the same, however, is not true for the copper content. Although it is generally agreed that in the beef heart enzyme the Cu/Fe ratio is close to 1 [32] and thus at least 2 copper ions are bound to the protein, several reports indicate that this ratio is sensibly higher than unity [33–35]. In 1984 and 1985 Einarsdottir and Caughey [36,37] found a slight excess of copper over the expected 1:1 Cu/Fe ratio using inductively-coupled plasma–atomic emission spectroscopy (ICP-AES, a technique which allows simultaneous metal determination to be made); stoichiometric amounts of zinc and magnesium were also found [35,36]. In 1987 Steffens et al. [30], using the same technique, extended the previous determinations to the enzyme from *Paracoccus denitrificans*. Moreover, since the sulphur content of COX is known from sequence analysis, its determination was included as an internal standard. Their result indicated a Cu/Fe ratio of almost 1.5, which would suggest the presence of three copper ions per mole of functional unit in both eukaryotic and prokaryotic COX. Recently protein engineering has shown the latter hypothesis to be correct.

1.4. Optical spectroscopy

Optical spectroscopy of COX is dominated by heme *a* transitions [1–3]. Notable differences relative to protoheme include: (a) substitution of a vinyl group in position 2 with a long isoprenoid (farnesyl)

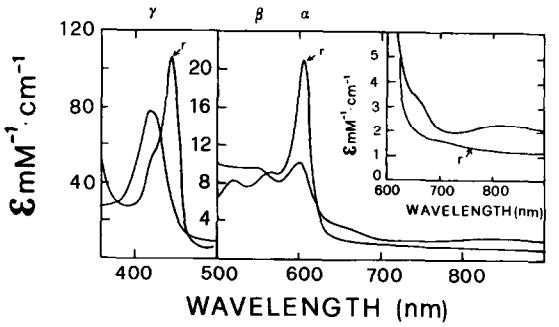

Fig. 2. Electronic spectra of fully reduced (r) and fully oxidised cytochrome *c* oxidase. The positions of the α, β and γ (Soret) bands are given above.

chain and (b) substitution of a methyl group in position 8 with a formyl residue. These differences reduce the heme symmetry and attenuate the extinction of the β-band of both cytochrome *a* and cytochrome a_3, while the α-band is intensified and red-shifted. The visible and near-infrared spectrum of COX purified from beef heart mitochondria in the oxidized and reduced states is shown in Fig. 2. The spectrum of the oxidized protein as purified (the so-called resting enzyme) is characterized by broad absorption bands, with peaks centred at 418–420 nm (the Soret or γ-band) and 598–600 nm (the α-band). Upon reduction of the enzyme (e.g. with sodium dithionite) the Soret band shifts to the red by as much as 26 nm, the molar absorbivity increasing by about 37%; the α-band shifts to 605 nm and doubles its extinction coefficient ($\epsilon = 12\ \mathrm{mM^{-1}\ cm^{-1}}$). The position of the Soret peak in the oxidized enzyme is particularly sensitive to the previous history of the protein and to the ligation state of cytochrome a_3 and in any case always shifts to the red.

It is now established that both cytochrome *a* and cytochrome a_3 contribute to these optical transitions, although with different amplitudes. On the basis of the differential reactivity of cytochrome *a* and cytochrome a_3 with ligands (only the latter binds exogenous ligands such as dioxygen, cyanide and carbon monoxide) and the possibility of preparing various half-reduced derivatives of COX, it has been possible to deconvolute the optical properties of the two cytochromes [6,38–40], with the generally verified assumption that the redox state of one cytochrome does not perturb the spectroscopic properties of the other (however, see [41]). Other distinc-

tive features of the oxidized enzyme are a broad low-extinction near-infrared band centred at 830 nm and a shoulder at 655 nm (inset to Fig. 2). The latter is thought to arise from the interaction between Cu_B and cytochrome a_3 [42]. Previous studies on the 830 nm chromophore have indicated that it is due (largely but not exclusively) to copper [43–45]; it is now believed that the EPR-detectable Cu_A(II) is, by and large, responsible for this transition.

1.5. Cu_A site

Recently the chemistry of the Cu_A site has been reconsidered in the light of important findings suggesting that the site contains 2 copper atoms instead of 1 [46], as classically believed.

Classic features: cupric copper, $3d^9$ electronic configuration and one unpaired electron, is usually found in proteins in tetragonal or distorted tetragonal ligand fields, with g values 2.0–2.4. However, the copper EPR signal of COX (Fig. 2) has no resolved hyperfines both at the X-band and Q-band (9 and 35 GHz, respectively) [32,35]. The line-shape is axial at X-band ($g_x = 2.18$ and $g_x = gy_z = 2.00$), but at Q-band displays rhombic splitting ($g_z = 2.18$, $g_y = 2.03$ and $g_x = 1.99$, the latter being lower than that for the free electron). The EPR signal is quite difficult to saturate at 93 K, a unique feature compared to low-molecular-weight Cu(II) complexes, protein-bound Cu or other blue Cu proteins. Treatment of COX with SDS drastically changes the EPR (see Fig. 3a and b), and completely bleaches the 830 nm charge-transfer band of Cu_A (not shown). The EPR-detectable copper Cu_A is of the type found in cupredoxins containing type I centers [47,48], i.e. with an unusually narrow parallel hyperfine coupling constant in the EPR spectrum ($A_{\|}$ is in the range 80–30 gauss and for Cu_A it must be < 30 gauss [49]). The similarity in the spectroscopic properties (although not stringent) is paralleled by homologies in the aminoacid sequence of the Cu-binding site [50]. As a matter of fact, regions of the primary structure of these proteins are homologous to the sequence of subunit II of beef heart COX, which is conserved in cytochrome c oxidases; this information strongly suggests that the binding site for Cu_A is on this polypeptide (see below).

According to Chan and coworkers [51–53], coordination of the copper(s) involves at least one Cys and one His (and possibly an additional Cys) from subunit II, based on spectroscopic (ENDOR) observations of COX from yeast grown with isotopically labelled His or Cys. X-ray edge absorption studies of Cu_A have indicated that the coordination charge at the Cu ion does not change appreciably upon reduction [54] and have established sulphur ligation to a copper atom [55–57].

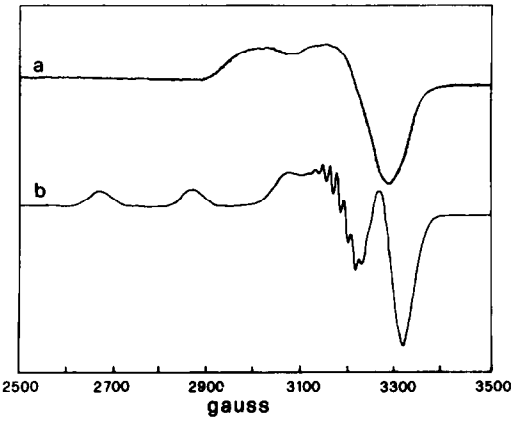

Fig. 3. X-band EPR spectrum of Cu_A. (a) Native Cu_A signal, double integration of the signal accounts for 0.8 Cu ions/functional unit; (b) sample a treated with 2% sodium dodecyl sulphate in air, line-shape typical of adventitiously bound copper ('biuret spectrum'). The intensity of the signal accounts for 2.2 Cu^{2+}/mol of enzyme (as compared to 0.8/mol in the native protein), indicating that in the native protein at least one copper ion is EPR undetectable. Conditions: $T = 90$ K; microwave frequency = 9.15 GHz; microwave power = 5 mW.

This description of the Cu_A site, however is not unanimously accepted: it is important to stress that among the 2 or 3 Cu ions bound per mole of functional unit, only (slightly less than) 1 is detected by EPR. Since a second copper ion (Cu_B) is undetectable because of its magnetic interaction with the Fe^{3+} of cytochrome a_3, the 'newly' discovered third Cu (see Table 1) has escaped detection by every spectroscopic technique, which has suggested the existence of novel copper clusters with peculiar spectroscopic properties [58].

The binuclear copper-site model: in 1988 Kroneck et al. [46] suggested that the Cu_A site is binuclear, and contains 2 copper atoms in a mixed valence state. Since then, this hypothesis has been supported by careful metal analysis yielding in several cases a 3Cu/2Fe stoichiometry, as well as by other indepen-

dent evidence, such as: (i) nitrous oxide reductase, the terminal acceptor of the electron transport chain in denitrifying bacteria shares some distinctive properties with COX [46,59–61]. One of the EPR detectable sites of this enzyme is a mixed valence copper dimer of structure [Cu(1.5) ... Cu(1.5)], whose EPR properties are very similar, though not identical, to Cu_A (the similarity being most obvious at C-band, 4 GHz of frequency); (ii) metal analysis and spectroscopy carried out on a Cu_A site recently engineered (mutagenesis experiments) in the C-terminal hydrophilic portion of subunit II of the *E. coli* quinol oxidase, naturally devoid of the Cu_A site, are confirmatory of the binuclear site model [62,63]; observations have been extended to the hydrophilic subunit II domain from *Paracoccus denitrificans* [64]. Though growing experimental evidence strongly supports the hypothesis of a binuclear Cu_A site, it is yet in doubt whether Cu_A is indeed a mixed valence binuclear site, see also [2]. As a matter of fact, it is observed that the second copper ion of the Cu_A cluster seems to resist reoxidation even upon denaturation (see Fig. 3); moreover Cu_A behaves as a single electron acceptor in the native enzyme. Thus in this review we shall only (and often) refer to four functionally significant metal centers.

1.6. Cytochrome a

Fe^{3+} with d^5 configuration can have $S = 5/2$ or $S = 1/2$, high- and low-spin, respectively. The ligand-field symmetry of low-spin ferric heme is typically rhombic and the EPR spectrum displays three g values ranging from 0.8 to 3.5. Cytochrome *a* falls in this category [32,33,35]. It is a bis-imidazolate low-spin center in both oxidation states II and III. The shape of the EPR signal and the EPR parameters ($g_x = 3.03$, $g_y = 2.24$ and $g_z = 1.45$) are typical of a magnetically diluted low-spin heme. The EPR spectrum of cytochrome *a* from beef heart COX is shown in Fig. 4. The signal intensity closely matches the protein concentration. The nature of the proximal and distal ligands has been elucidated on the basis of comparison with the resonance Raman [65,66] and the magnetic circular dichroism [67,68] of model compounds. The heme of cytochrome *a*, although easily accessible for electron transfer, is likely to be buried within a hydrophobic pocket due to its long isoprenoid side chain.

1.7. Cytochrome a_3–Cu_B site

The Fe of cytochrome a_3 and Cu_B are very close (≤ 5 Å) to one another, and form a magnetically coupled heterobinuclear center. The result of this interaction is the lack of EPR signals from the individual metals even in the oxidized state. It has been shown by magnetic susceptibility experiments [69,70] and MCD spectroscopy [71] that cytochrome a_3 (Fe^{3+}, $S = 5/2$) and Cu_B (Cu^{2+}, $S = 1/2$) are strongly antiferromagnetically coupled (as in type-III binuclear copper centers [48]) to form an $S = 2$ spin system which, using ordinary EPR instrumentation, cannot be detected. As a possible alternative, the oxidized resting cytochrome a_3–Cu_B center may contain a ferryl ion [Fe(IV)] coupled to a Cu(I) site [72]; this would provide a structural basis for the CO-driven reduction of this site yielding the mixed-valence species [73,74], a derivative of COX in which cytochrome *a* and Cu_A are oxidized and the cytochrome a_3–Cu_B site is reduced (ferrous–cuprous) and in combination with carbon monoxide. Fe(IV) may, indeed, be generated during one-turnover experiments [75] (in the form of an oxo–ferryl ion) and is suitable for reaction with carbon monoxide, the Fe(IV) being a two-electron acceptor. This proposal, however, should be contrasted with recent Mössbauer experiments on beef heart and *Thermus thermophilus* COX, which support the classical view of a high-spin ferric cytochrome a_3 in the resting (i.e. as purified) oxidized state [76].

The oxidized beef heart enzyme always displays a low-intensity, high-spin ($g = 6$) EPR signal [32].

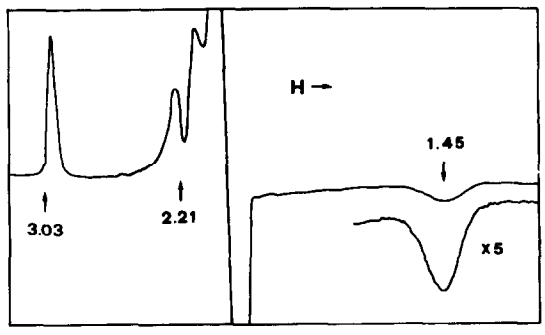

Fig. 4. EPR spectrum of ferric cytochrome *c* oxidase showing the low-spin heme *a* signal. Conditions: $T = 16$ K; microwave frequency = 9.15 GHz; microwave power = 2 mW. Modified from [35] with permission.

This signal may be due to partial autoreduction (possibly of Cu_B?) since it is suppressed by addition of ferricyanide or is transiently increased following addition of cytochrome *c* and ascorbate (under these conditions, the signal accounts at most for 23% of the expected intensity) [35].

The spectroscopic properties of cytochrome a_3 and Cu_B have been studied by selective reduction experiments. Since the lack of EPR signals is due to the strong coupling of the two metal spins, by preferential reduction of one of the two metals the interaction is disrupted and the oxidized partner in the binuclear center may therefore exhibit an EPR signal, as shown by Stevens et al. [77]. In this investigation NO (which bears one unpaired electron) was added to a strictly anaerobic solution of oxidized beef heart COX. While no changes in the EPR signal of either cytochrome *a* and Cu_A were observed, a rhombic high-spin EPR signal was generated by this treatment ($g_x = 6.16$, $g_y = 5.82$, g_z being obscured by the Cu_A signal) and its intensity accounted for approximately 60% of one heme (the amount being preparation-dependent). This classical experiment, which is shown in Fig. 5, demonstrates that the high-spin $g = 6$ signal arises from cytochrome a_3, since addition of NO to the oxidized protein breaks the antiferromagnetic coupling between the Fe(III) and the Cu(II), by reducing the latter metal exclusively.

The presence in oxidized resting oxidase of a ligand bridging cytochrome a_3 and Cu_B, and thereby

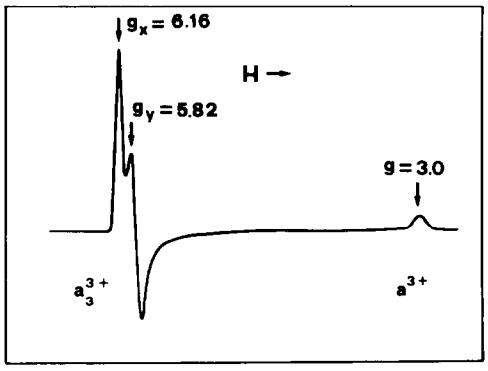

Fig. 5. EPR spectrum of cytochrome a_3, obtained following addition of nitric oxide (to a pressure of 0.95 atm) to anaerobic oxidised cytochrome *c* oxidase. Conditions: $T = 7$ K; microwave frequency = 9.16 GHz; microwave power = 0.2 mW. Modified from [77] with permission.

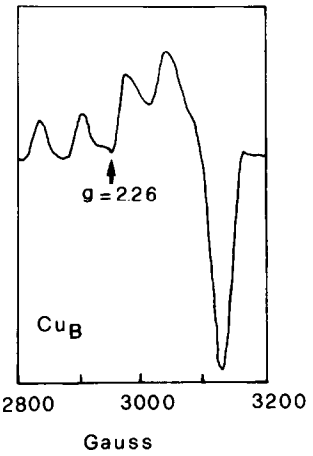

Fig. 6. Cu_B EPR spectrum observed after incubation of an initially fully reduced cytochrome *c* oxidase sample for 45 s at 191 K in the presence of O_2. Conditions: $T = 9$ K; microwave frequency = 9.17 GHz; microwave power = 0.2 mW. Modified from [75] with permission.

mediating magnetic exchange interaction between the two metals, has been amply discussed; EXAFS studies have proposed a sulphur atom as the bridging ligand [78]. Since the binuclear center is located in subunit I (see below), where no invariant cysteines are available (but methionines are), the assignment of the bridging ligand has been actively debated. Other Fe-EXAFS experiments performed on a Cl-depleted COX preparation [79] indicate that the intensity of the peak attributed to the bridging sulphur (which EXAFS cannot distinguish from Cl) is substantially attenuated. This result would seem to indicate that the bridging ligand is a Cl^- ion, whose function, if any, remains to be established.

Reoxidation of fully reduced COX with dioxygen in the presence of cytochrome *c* led to the discovery [80] of a new type-II Cu signal, detected as a transient (see Fig. 6). This signal is clearly rhombic ($g_z = 2.278$, $g_y = 2.109$, $g_x = 2.052$) and was assigned either to oxidized Cu_B with cytochrome a_3 in the reduced state (no $g = 6$ signal was present in some preparations), or to a Fe(IV)–oxo complex originating after the cleavage of the O–O bond of dioxygen [81]. Further experiments on this intermediate [75,82] have demonstrated that this rhombic Cu_B signal arises from an intermediate in which ferrous (low-spin) cytochrome a_3 is ligated either to carbon monoxide or dioxygen (see also Section 2).

These experiments suggest that reduction of Cu_B by the cytochrome a–Cu_A sites is faster than the reduction of cytochrome a_3 (see page 98 of [3]) since the Cu_B-EPR signal cannot be detected under (reducing) equilibrium conditions.

Studies of the NO complex of reduced cytochrome a_3 [83,84] have indicated that the fifth ligand of the heme Fe of cytochrome a_3 is a nitrogen. After incorporation of ^{15}N-histidine in the enzyme from yeast, an histidine residue could be unambiguously identified as the fifth endogenous ligand to cytochrome a_3 [85]. Finally, Cu ENDOR spectra of COX indicate the presence of three distinct nitrogenous ligands of this metal; of these, at least one is a histidine. This result established the similarity between Cu_B and the type-III Cu site found in laccase [48,80,81]. A very unusual transient EPR signal is observed when reduced COX is rapidly mixed with dioxygen ($g = 5$, 1.78, 1.69) [86,87]. As discovered by Antonini et al. [88], the so-called *pulsed* oxidase is a conformational state of the enzyme generated within milliseconds after mixing the fully reduced enzyme with excess dioxygen; after oxidation, *pulsed* oxidase decays back to *resting* with half-times of many seconds to minutes. Experiments with $^{17}O_2$ provided no evidence of oxygen being involved in the structure of this intermediate [89], in complete agreement with kinetic data showing that the pulsed state can be populated by oxidation with oxidants other than oxygen (see [1] for discussion and references).

In addition to the four 'canonical' redox-active metals, it appears that one functional unit of COX also contains one Zn atom [30,36,37]. An investigation carried out by EXAFS [90] indicated that Zn is in a distorted tetrahedral environment and is coordinated to three S and one N; this would seem to place this metal, with hitherto unknown function, in one of the cytoplasmatically synthesized subunits.

1.8. Location of the metals

For a more detailed description of the techniques and experiments carried out to determine the location and ligation state of the metals in COX see [91,92]. Here we describe only the currently accepted and emerging picture. Important clues to the localization of metals have come from the study of bacterial cytochrome oxidases, such as *Paracoccus denitrificans* or *Rhodobacter sphaeroides* proteins. These bacterial oxidases contain 2 heme a groups (a and a_3) and 2 copper atoms, and their spectroscopic and functional properties are remarkably similar to those of the eukaryotic enzyme. Nevertheless, the enzyme from *Paracoccus denitrificans*, as originally purified, is made up of only two subunits (I and II) [6,7] which are chemically and immunologically related to the corresponding eukaryotic subunits; also subunit III [93] is present but this polypeptide is somewhat loosely bound and thereby was lost in the initial purification procedure (see also [24]). Thus the four canonical redox-active metals must reside on subunits I and II.

General consensus places the Cu_A site in subunit II as proposed originally by Steffens and Buse [50] on the basis of sequence homology between residues 161 and 207 of subunit II (from beef heart COX) and the active site of azurins. The quinol oxidase from *Escherichia coli* (i.e. cytochrome *bo*) [94] does not contain a Cu_A site, though capable of redox-linked proton translocation [95–97]. Nevertheless it was possible to demonstrate by genetic engineering experiments that a cupredoxin-like motif is present in this protein, which undoubtedly strengthens the proposed structural homology with both the cupredoxins and COX. A Cu_A-binding site in subunit II of the quinol oxidase from *E. coli*, which is naturally devoid of Cu_A, is presently being engineered by genetic methods [98].

The two cytochromes and Cu_B are in subunit I, as shown unequivocally by the properties of *Paracoccus denitrificans* COX and analysis of invariant residues acting as metal ligands in subunit I. This has been recently demonstrated by the elegant site-directed mutagenesis experiments of the group of Ferguson-Miller et al. [99,100]. In this case, the three-subunit a_3-type COX of *Rhodobacter sphaeroides*, which is structurally and functionally homologous to mitochondrial and *Paracoccus denitrificans* COX, have been expressed and mutated. Subunit I contains six totally conserved histidine residues, as found from sequence comparison between several species. Alfa-helix membrane-spanning propensity calculations are consistent with 12 transmembrane helical spans, as also found for bovine subunit I. Each of these conserved histidines was mutated and the ef-

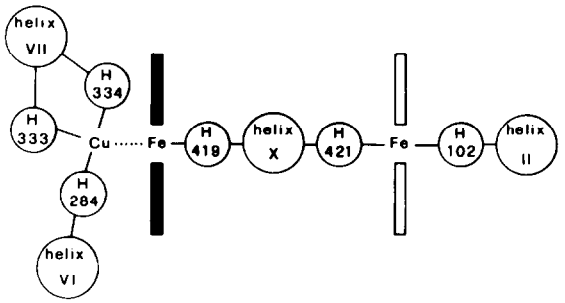

Fig. 7. Proposed structure of the metal sites bound to subunit I. Vertical bars represent heme *a* (open) and heme a_3 (closed). Cu_B is also shown. Modified from ref. [100] and [109].

fect on the spectroscopic properties (visible and resonance Raman spectroscopy) examined. In conclusion, cytochrome *a* and the cytochrome a_3–Cu_B sites are located in subunit I, where they are presumably buried inside the protein and within the lipid bilayer; the possible ligands to these metals from subunit I, as proposed by [99,100], are shown in Fig. 7. It is interesting to notice that 4 transmembrane helices (II, VI, VII, X) contribute the ligands of these three metals, and that from the latest model cytochrome *a* and the binuclear center are located almost at the same level within the membrane. The proximal histidine of cytochrome a_3 (His 419) is on helix X and only 2 residues downstream from His 421, one of the two axial ligands of the (low spin) cytochrome *a*. Cu_A, on the other hand, is ligated by residues found in subunit II in a structural domain, topologically located on the cytoplasmic side of the biomembrane, which recalls that of cupredoxins. As shown below and already alluded above, oxidases can be fully functional even in the absence of Cu_A, which therefore plays no unique role in these enzymes.

2. Electron transfer processes

2.1. Introduction

The reaction catalysed by cytochrome *c* oxidase is shown in Eq. (1):

$$4c^{2+} + 4H^+ + O_2 \rightarrow 4c^{3+} + 2H_2O \qquad (1)$$

where four ferrocytochrome *c* molecules transfer electrons (one at the time) to COX, and O_2 is reduced to H_2O. The electron entry site(s) (cytochrome *a*, Cu_A or both, see Section 1) is structurally and topologically different from the binuclear site (the cytochrome a_3–Cu_B site) where binding and reduction of dioxygen takes place; thus, electrons are transferred intramolecularly through the protein from the former sites to the latter via unimolecular eT processes, which will be described below (see Sections 2.4 and 2.5). Eq. (1) applies not only to the enzyme as isolated in detergent solution, but also when COX is embedded in native or artificial membranes. In the latter conditions it is possible to demonstrate the redox-linked proton translocation activity of COX, as shown by Wikström in 1977 [4], whereby vectorial proton movements are coupled to the transmembrane eT processes (see Section 3).

It is important to stress, as a final introductory note, that the reaction catalysed by COX is essentially irreversible, due to the O_2 reduction, and more specifically to two processes involving eT to O_2 already bound to the binuclear center (see Section 2.6).

2.2. Conformations

Resting and pulsed: since their discovery [88], these terms designated two conformations of the enzyme characterized respectively by a slower or faster turnover rate. Typically resting oxidase is the species obtained when preparing the enzyme following Yonetani's procedure [7], which includes an acidification step to collect mitochondrial membranes (see below the slow and fast conformations), while pulsed oxidase is generated by exposing fully reduced oxidase to oxygen [88,101]. The specific activity of the pulsed enzyme is always greater by a factor which, depending on experimental conditions and history of the enzyme, may vary from 2 to 10 [102]. This variability has been proposed to depend on the fact that resting oxidase may be a mixture of various conformational states produced (somewhat artefactually) during enzyme purification, for reasons still not fully understood [103]. The catalytic activity of oxidase was more than puzzling, given that the resting enzyme displays an unusually slow rate of reduction of the bimetallic site, and polyphasic cyanide binding kinetics [104,105]. On the contrary pulsed oxidase binds cyanide monophasically, and its

turnover number is more compatible with the internal electron transfer rate; under the best conditions (reconstituted in uncoupled vesicles) it may be as high as 100 s^{-1} or more [106], a figure lower but not inconsistent with the catalytic rates observed using mitochondria. It has been shown that the resting to pulsed transition is a reversible process which can be induced in both directions, and it was observed not only with the soluble but also with the vesicle-reconstituted enzyme [107], and with submitochondrial particles, at least in those preparations which include an acidification step [108]. The original kinetic findings [88,101] together with more recent observations [109,110] suggest the resting to pulsed transition to be related to structural changes possibly of the binuclear center, affecting ligand binding and internal electron transfer from the electron accepting pole to the oxygen binding site.

Spectroscopically, the oxidised resting conformation is characterized by a blue shifted absorption band in the Soret region, a $g = 12$ EPR signal (assigned to the binuclear center). The oxidised pulsed conformation displays a 420–421 nm absorption band and a new $g = 5$, 1.78 and 1.69, EPR signal; those features are extensively reviewed elsewhere [13].

Slow and fast: Baker et al. [105] observed that changing the purification procedure of cytochrome oxidase starting from that introduced by Hartzell and Beinert, a form of the enzyme able to react with cyanide in a single phase was isolated. This form was converted into a slowly reacting species by exposing the enzyme to low pH (below 7.0) or (as demonstrated later) following incubation with anions such as formate [111]. The two forms have been called, since then [105], 'slow' and 'fast', to be distinguished from resting and pulsed basically because of the different experimental protocol used to generate them. Comparison of the basic spectral and functional properties of 'resting' vs. 'slow' and 'pulsed' vs. 'fast' forms suggests that these definitions can be thought as synonymous [111]. However the finding that the pulsed state slowly reverts to resting while the 'fast' does not (to 'slow') perhaps indicates a difference between the two species [105].

Open and closed: the kinetic properties of the fast enzyme may reasonably account for turnover rate. However, as originally observed by [104,112,113]

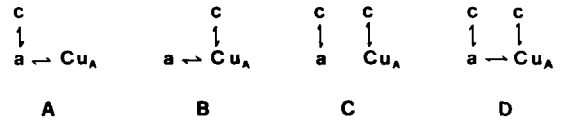

Fig. 8. Electron entry mechanisms.

and later on clearly pointed out by [111] the rate of cyanide binding even to 'fast' oxidase is dramatically slower (several orders of magnitude) than the rate accounting for onset of inhibition during turnover. Thus it has been proposed [112] that a state populated only during turnover (most probably mixed valence) is competent for very rapid binding and called 'open' [113]; by definition, all the other conformations are therefore 'closed' [113]. The 'open' to 'closed' transition may also be related to general models for proton pumping, as in the 'closed' state protons may be uptaken by the enzyme and released vectorially in the 'open' state [114]. The correlations between the present consensus structure of the oxidase's active site and the reactivity towards cyanide of a one-electron reduced enzyme has been dealt with by Wilson et al. [115].

2.3. Electron entry kinetics

The mechanism of electron entry into cytochrome oxidase has not been finally established, in spite of numerous studies [101,116–119]. It is known that the metals to which ferrocytochrome *c* will donate electrons are either cytochrome *a* or Cu_A or both. Fig. 8 schematically depicts the four possible kinetic schemes for the eT processes from ferrocytochrome *c* to COX; up to date no definitive experiment has

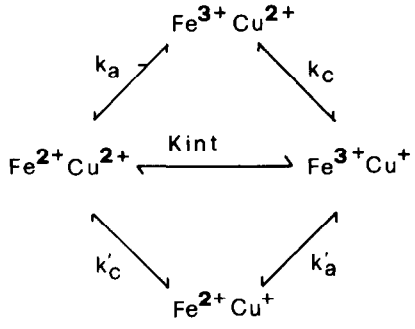

Fig. 9. General electron entry mechanism.

been presented to prove that one of the two prosthetic groups is the unique electron-entry site. A general mechanism is also presented in Fig. 9.

From a kinetic point of view, the reaction of cytochrome *c* with oxidase has been extensively studied, both at steady state and by transient kinetic techniques. Once ferrocytochrome *c* and oxidized COX are mixed, spectral changes in the millisecond time scale are observed at wavelengths monitoring ferrocytochrome *c* (550 nm) and cytochrome *a* (605 nm); similar results are obtained if reduced cytochrome *c* is generated from ferricytochrome *c* by pulse radiolysis [120], or if reduced COX is mixed anaerobically with ferricytochrome *c* [121]. These changes indicate rapid electron transfer from (or to) cytochrome *c* with reduction (oxidation) of cytochrome *a*, the reaction being concentration-dependent, with a rate constant which tends towards diffusion-controlled values at neutral pH and low ionic strength (ca. 5×10^8 M^{-1} s^{-1}), and decreases with increase in ionic strength (5×10^6 M^{-1} s^{-1}, in 0.1 M phosphate buffer, pH 7). The cytochrome *c* concentration dependence of the reaction is linear up to approximately 2000 s^{-1}, as followed by standard stopped-flow and temperature jump techniques, and no evidence for a rate limiting process at high protein concentration is detected [122] (but see below). Therefore: (i) electron transfer within the collisional complex must be very fast compared to binding; (ii) since more than one electron acceptor is being reduced during the burst phase of the reaction (i.e. during the first 10 ms), the ferricytochrome *c* off-rate cannot be rate-limiting, if two eT pathways are excluded. This applies also to the derivatives of cytochrome oxidase in which the cytochrome a_3–Cu_B site is stabilized in its higher oxidation state (ferric/cupric) by ligands (such as cyanide and azide), or in its lower oxidation state (ferrous/cuprous) by CO (the so-called mixed-valence CO derivative). Thus, the initial eT events are insensitive to the redox state of cytochrome a_3, whether unliganded, or liganded with cyanide, azide or carbon monoxide, though the redox potentials of cytochrome *a* and Cu_A are generally thought to be quite different in these derivatives. See Table 1 and [123–126] for a compilation of apparent second-order rate constants for reduction of COX by cytochrome *c* and other reductants.

The differential equations which describe the four electron entry mechanisms shown in Fig. 8 all predict the following [127]:

$$d[c^{3+}]/dt = d[a^{2+}]/dt + d[Cu_A^+]/dt \quad (2)$$

$$\left(d[c^{3+}]/dt\right)_{t=0} = \left(k_a + k_{Cu_A}\right) * \left[a^{3+}Cu_A^{2+}\right] * [c^{2+}] \quad (3)$$

$$\left(d[a^{2+}]/dt\right)_{t=0} = k_a * \left[a^{3+}Cu_A^{2+}\right] * [c^{2+}] \quad (4)$$

Eq. (2) states that all times the rate of formation of ferricytochrome *c* is exactly balanced by the sum of the rates of reduction of cytochrome *a* and Cu_A, even if the former were reduced in a bimolecular mode and the latter by a monomolecular process internal to the protein (see below). Eqs. (3) and (4)

Table 1
Second-order rate constants for reduction of cytochrome oxidase

Reductant	k (M^{-1} s^{-1})	Electron acceptor	Technique [a]	Ref.
Cytochrome *c*	$10^7 - 10^8$	*a*	SF	[101,116–119]
	6.0×10^7	*a*	PR	[120]
	9.0×10^6	*a*	TJ	[122]
Porhyrin cytochrome *c*	2.0×10^7	*a*	PR	[123]
Dithionite	4.0×10^5	*a*	SF	[124]
$Ru(NH_3)_6^{2+}$	5.0×10^5	*a*	SF	[125]
	1.5×10^6	*a*	SF	[126]
MNA radical [b]	1.5×10^9	Cu_A	PR	[140]
Ru^{2+} complex excited state [c]	–	Cu_A	FP	[141]

[a] SF = stopped-flow; PR = pulse radiolysis; TJ = temperature jump; FP = flash photolysis.
[b] 1-Methylnicontiamide radical.
[c] tris(2,2′-Bipyridyl)ruthenium(II). Initial phase not resolved, but complete in < 1 μs.

predict that if two independent electron acceptors are present in COX, it must be verified that the *initial* rate of oxidation of ferrocytochrome *c* exceeds the initial rate of reduction of cytochrome *a* (in Eqs. (3) and (4), where k_a and k_{Cu_A} are the bimolecular rate constants for reduction of cytochrome *a* and Cu_A, respectively).

Among the most intriguing aspects of the cytochrome *c*–cytochrome oxidase interaction is the nature and location of the substrate binding site. Upon mixing oxidized cytochrome oxidase with ferricytochrome *c* at low ionic strength it is possible to isolate a 1:1 electrostatic complex [128] ($K_D = 10^{-8}$ M, with an off-rate of the order of 0.1 s^{-1} or lower). This binding site on COX involves subunit II, close to the putative Cu_A binding site; the physical basis of the interaction lays on the presence on cytochrome *c* and subunit II of complementary charges, which are involved in stabilizing the electrostatic complex (see [92] and references cited therein). This complex can be 'frozen' by covalent crosslinking using carbodiimides [129–132] or arylazido–cytochrome *c* [133]. The cytochrome *c* binding site is complex involving, as it does, also subunit III, as shown by crosslinking experiments of cysteine-107-thionitrobenzoate modified yeast cytochrome *c* [134,135] to cysteine 115 of subunit III in beef heart COX [136]. The interpretation of these results [137] suggests that cytochrome *c* binds to dimeric COX in a cleft delimited by subunit II of one monomer and by subunit III of the other. Since also cytochrome *a*, which is located in subunit I, takes part in the initial eT events, this subunit as well must be part of the cytochrome *c* binding domain.

The effect of ionic strength on the reduction of oxidized bovine COX by cytochrome *c* was studied by a laser photolysis technique [138]. In these experiments a laser pulse generates a flavin semiquinone radical (5-deazariboflavin) in a very short time (< 1 μs). When the photolysis is carried out in the presence of COX, cytochrome *a* is only poorly reduced despite the very large driving force (ca. 1 volt). When, however, the experiment is carried out in the presence of ferricytochrome *c*, monophasic reduction of cytochrome *a* is observed while the kinetics of cytochrome *c* oxidation is multiphasic, the rate constant of the fastest process being identical to the rate constant of reduction of cytochrome *a*. Moreover,

$$F^{\cdot} + c^{3+} \xrightarrow{k_c} F + c^{2+}$$

$$c^{2+} + a^{3+} \underset{k_{-1}}{\overset{k_c}{\rightleftarrows}} c^{2+}\text{–}a^{3+}$$

$$c^{2+}\text{–}a^{3+} \xrightarrow{k_{eT}} c^{3+} + a^{2+}$$

Scheme 1.

during the fastest phase, 2 equivalents of cytochrome *c* are oxidized per heme reduced [101,116–119,127], and the concentration dependence of the rates is hyperbolic [119]. The initial rates of cytochrome *c* oxidation and cytochrome *a* reduction appear to be very similar, an indication that with cytochrome *c*, cytochrome *a* is the unique electron acceptor. The early events of eT to cytochrome *a* are interpreted [138] according to Scheme 1, where $F^{\cdot}$ and F correspond to the semiquinone and oxidized flavin species, respectively; $k_c = 10^9$ M^{-1} s^{-1}, $k_1/k_{-1} = 5 \times 10^4$ M^{-1} and $k_{eT} = 1600$ s^{-1} (at $I = 110$ mM) in the above model represents either the ferricytochrome *c* off-rate or the eT process within the collisional complex. The ionic strength dependence of this process has yielded important information on the nature of the electron entry site. Since the interaction is essentially electrostatic, it is expected that at higher ionic strengths the efficiency of eT should be impaired. It is found, however, that formation of the strong electrostatic complex at low ionic strength is not coincident with the most efficient eT rate; rather, the fastest eT occurs at ionic strengths (0.11 M) at which the complex with cytochrome *c* is considerably weakened, as also appears for the cytochrome *c*–cytochrome *c* peroxidase electrostatic complex (in both cases the ionic strength dependence of k_{obs} is bell shaped). Therefore if cytochrome *c* binds close to the Cu_A site then: (i) the orientation of the two redox metals is not optimal for eT to occur, especially if the ionic strength of the aqueous medium is high as in the mitochondrial intermembrane space (ca. 0.2 M), and (ii) the previously estimated rates for ferricytochrome *c* dissociation (0.1 s^{-1}) are not applicable to the turnover situation, since at high cytochrome *c* concentrations typical rates of 200 s^{-1} are observed.

Cu_A modification and depletion after treatment of COX with mercurials (*p*-hydroxymercuribenzoate) [127,139] has shed some light on the role of the metal centers in the initial events of eT from cy-

tochrome *c*. In this derivative, Cu_A is removed either physically or functionally. In the latter case it was shown that Cu_A has changed to a type II site, with a decrease of the redox potential by as much as 150 mV [142]; thus, cytochrome *c* would no longer be able to reduce this metal. Using this derivative it was shown that the burst stoichiometry was significantly decreased as compared to the control (1.3 vs. 2.0 electrons/functional oxidase unit) [127]. Analysis of the functional dependence on cytochrome *c* concentration in terms of Scheme 1 [143] (see above), yields identical constants for control and Cu_A-depleted cytochrome oxidase (5.4 and 5.0×10^4 M^{-1}, respectively), indicating that Cu_A depletion has not disrupted complex formation. On the other hand, the rates of intracomplex eT were quite different (k_{eT} in Scheme 1: 2580 and 740 s^{-1}, for native and Cu_A-depleted oxidase, respectively). It is important, however, to recall that COX (from beef heart) contains 17 cysteine residues [144] that may react with the mercurial; in the above studies it was tacitly assumed (but not proven), that none of these residues is critical for the initial and subsequent eT processes.

Steady-state experiments using a covalent derivative of COX with stoichiometric cytochrome *c* crosslinked to the high affinity site [145] indicate that crosslinked cytochrome *c* is not transferring electrons to the site to which it is bound (presumably close to Cu_A). Though oxidation of exogenously added cytochrome *c* is sterically hindered, the results are consistent with the idea that efficient eT from exogenous cytochrome *c* occurs also with cytochrome *a*. In the crosslinked complex either the redox partners are not optimally 'tuned' for efficient eT to occur, or the crosslinking procedure affects some residues relevant to the eT process from covalently linked cytochrome *c* to Cu_A.

The overall picture which has emerged from the above indicates that cytochrome *a* is a bona fide electron acceptor site, thus models B and C in Fig. 8 may be excluded. This view, however, is not completely agreed with. Firstly, Kobayashi et al. [140] have shown, using a 1-methylnicotinamide radical generated by pulse radiolysis, that Cu_A is very rapidly and preferentially reduced with a second order rate constant of 1.5×10^9 M^{-1} s^{-1} (see Table 1). Secondly, generation by flash photolysis of the strongly reducing excited state of tris(2,2′-bipyridyl)ruthenium(II) at low ionic strength [141] also indicates preferential reduction of Cu_A on a < 1 μs time scale (though very high concentrations of aniline are present) (Table 1). Thirdly, the results of the flow–flash experiments of Hill [146] show that the fastest phase of reoxidation of Cu_A in the initially fully reduced COX is blocked by cytochrome *c*, whereas the effect of the substrate on cytochrome *a* reoxidation appears only at later times. In conclusion, from what has been discussed above it is possible to exclude only model B in Fig. 8 as a candidate for the mechanism of electron entry in cytochrome oxidase.

Table 2
Redox potentials of the metal centers in COX

Metal	E_0 (mV)						
a	330–380	220	220	340	276	330–350	275
Cu_A	220–240	240	245	285	288	–	–
a_3	205–220	340	385	350	–	270–312	–
Cu_B	340	340	345	225	–	–	–
State [a]	O	O	O	O	MV	O	MV
Ref.	[147]	[148]	[149]	[150]	[151,152]	[153]	[153]

[a] O = Oxidized, MV = mixed valence + CO.

Once an electron has entered into cytochrome oxidase via cytochrome *a* and/or Cu_A, it is rapidly shared with the partner metal (see horizontal line in Fig. 9 connecting the a^{2+} Cu_A^{2+} and a^{3+} Cu_A^{1+} species). The observed rates should depend on the specific derivative of COX (oxidized, reduced, CO- or cyanide-ligated) since the redox potentials of the metals, as determined by static potentiometry, are derivative-dependent (see Table 2 and ref [147–150] for a compilation of the redox potentials). In general reduction of cytochrome *a* is favoured over Cu_A in the oxidized enzyme (rates of the order of 10^3–10^4 s^{-1} [140,141]) indicating that the redox potential of Cu_A must be lower than that of cytochrome *a*. The situation is reversed in the carbon monoxide mixed valence species where the redox potential of cytochrome *a* is slightly lower than that of Cu_A [151–154]. It is important to stress that the redox potential of cytochrome *a* in the CO derivative is ca. 80 mV lower than in the fully oxidized enzyme (see Table 2). This observation has been interpreted in terms of a conformational model (based essentially on the neo-classical hypothesis [155,156] which has profound consequences with respect to the steady state

and the proton pumping activity of cytochrome oxidase [157], according to which electron input (high potential cytochrome *a*) and output (low potential cytochrome *a*) enzyme states are sequentially populated during turnover, depending on the redox state of the binuclear site (specifically of Cu_B [158]), oxidized and reduced, respectively. If the (photolysed) CO derivative of COX is a good model analogue for the mixed valence species which (to some extent) is present under steady-state conditions, it must be argued that its interaction with ferrocytochrome *c* should be less favoured (the equilibrium constants for interaction with cytochrome *c*, with $E_0 = 260$ mV, would be ca. 33 in the oxidized enzyme and 2 in the CO derivative). As discussed above, however, the kinetics of eT to cytochrome *a* are largely insensitive (both in rates and amplitudes) to the redox and ligation state of the binuclear site [101,117–119], and the apparent equilibrium constant for eT between cytochrome *c* and cytochrome *a* lies in the range 2–4 (at room temperature and 0.1 M phosphate buffer [101]); thus there must be an important gap between the thermodynamic and kinetic interpretations of the data.

The reason for this discrepancy is not understood, but may be identified either in the existence of slow structural changes which occur with some states (e.g. resting) of COX, or in a limited applicability of the Nernst equation. As to the latter point (see D. Walz [159] and M. Denis, personal communication).

2.4. Some general considerations

The cytochrome a–Cu_A to cytochrome a_3–Cu_B eT processes (in the absence of O_2) will now be discussed. Each of the four canonical redox metals of COX may accept/donate one electron; thus, 4 sites with 2 accessible states (i.e. oxidised and reduced, ferric/ferrous or cupric/cuprous) will yield $4^2 = 16$ possible species which are schematically shown on the left-hand side of Fig. 10.

The species labelled by asterisks (species 11, 14, 15 and 16) are expected to bind and reduce molecular oxygen to different extents, though their population will be quite different depending on their formation and dissipation rates, which are also coupled to the reductant and O_2 concentrations. Up to date the distribution of the species concentrations as a function of the reductant concentration (solution potential) is unknown. This is due both to the uncertainties in the spectral contributions of the four known chromophores and possibly to spectral interactions among the sites [41].

The distribution of electrons shown on the left-hand side of Fig. 10 will be referred to as the 1:4:6:4:1 electron distribution. The electron distribu-

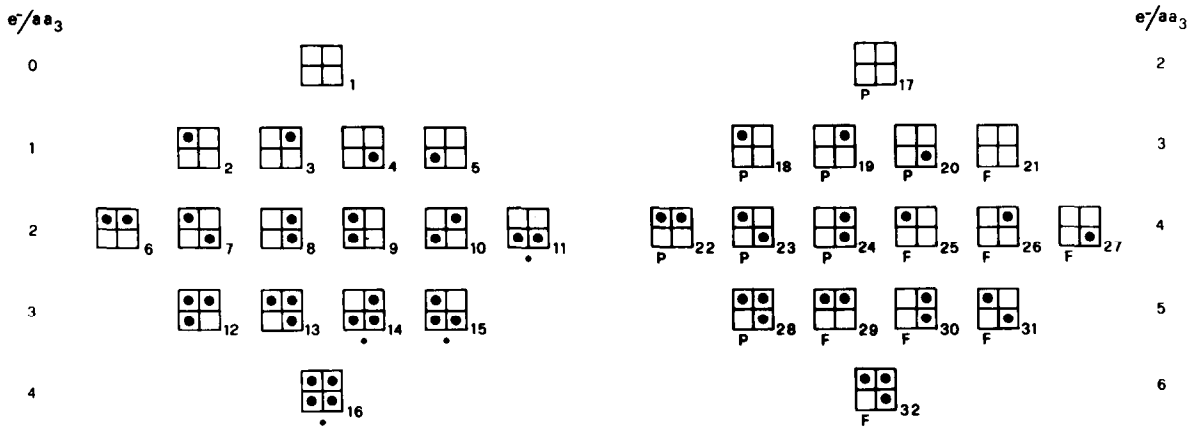

Fig. 10. The 1:4:6:4:1 electron distribution of COX. In this scheme the oxidase functional unit is depicted as a square containing four boxes which represent, in clockwise order and starting from the upper left box, cytochrome *a*, Cu_A, Cu_B and cytochrome a_3, respectively. Reduction is indicated by a dot, and all species are numbered for convenience. Each row (from top to bottom) represents the overall reduction level, e.g. there is 1 species carrying 0 electrons, 4 carrying 1, 6 carrying 2, etc. In the left-hand part, P and F-labelled species indicate COX species with partially reduced O_2 intermediates bound to the cytochrome a_3–Cu_B site. See text for further details and discussion.

tion between these four sites is governed by their respective redox potentials and by the equilibrium reductant concentration the solution potential). Since it is known that the four sites mutually interact (see [153] for the interaction network), a complete description of the system would require 32 standard redox potentials. Assuming reversible reciprocal interactions, i.e. that the interaction potential between site i and site j is the same regardless of the redox state of the remaining sites in all possible permutations, the number of parameters reduces to 10 [160]: four 'upper asymptote' redox potentials, defined as the redox potential of site i when all the partner sites are oxidized, and six interaction potentials (d_{12}, d_{13}, d_{14}, d_{23}, d_{24}, d_{34}) whose magnitude determines the extent of the interaction between the sites and whose sign determines the *type* of interaction, i.e. whether cooperative or anticooperative, the latter applying to the case of COX); see [139] for a complete computational procedure or [161] for an alternative approach. To describe the monomolecular eT processes shown in Fig. 10 from a kinetic point of view, 48 microscopic rate constants forward and reverse directions) are needed, which are equally distributed between the following six processes:

$a \leftrightarrow Cu_A$ observed (1)

$a \leftrightarrow Cu_B$ inferred (2)

$a \leftrightarrow a_3$? (3)

$Cu_A \leftrightarrow Cu_B$? (4)

$Cu_A \leftrightarrow a_3$? (5)

$Cu_B \leftrightarrow a_3$ inferred (6)

Removal of the reverse rates would greatly simplify the overall scheme; under specific experimental conditions this is possible when a trapping non-reducible ligand is present (such as CO, see Section 2.5). It is nevertheless possible to simplify the scheme (to 36 monomolecular processes) if one considers that oxidized Cu_B has only been observed during an oxidative process [75,80–82] and not vice versa. In other words, during turnover, but also in one-turnover experiments, the internal eT to the binuclear site reduces Cu_B first. Thus, it would be possible to exclude monomolecular processes (3) and (5), which demand direct eT between the cytochrome a–Cu_A sites and cytochrome a_3, at least in the first half of the catalytic cycle (but see Section 2.6).

However, in view of the partial reversibility of the COX reactions under highly oxidizing conditions in mitochondria [97,162–164] or in the photolysed carbon monoxide mixed-valence derivative [166,167], and that the internal reverse eT between the binuclear site and the cytochrome a–Cu_A sites may determine the apparent rate of reduction of cytochrome a_3 and its O_2 dependence are clear indications that the reverse reactions in cytochrome oxidase may be crucial features.

In any case it is clear that the mechanism of cytochrome oxidase is very complex; even more so when taking into consideration the association of some kinetic processes to proton binding (not shown in Fig. 10) and the coupling to its uphill transport across the biological membrane.

One crucial aspect of the COX reaction is the identification of the rate-limiting step in catalysis. We may discuss this point with reference to the simplest scheme involving eT processes with the two substrates, i.e. cytochrome c and dioxygen, and eT processes within COX. The evidence suggests that the former events are not rate-limiting under turnover conditions, since the relevant rate constants are both close to diffusion-controlled. Thus the rate-limiting step must be internal to the protein, either product dissociation (ferricytochrome c) and/or internal intersite eT process. As already discussed in Section 2.3 product dissociation appears not to be the rate-limiting process because of the following: (i) at low ionic strength the off-rate of ferricytochrome c in the electrostatic complex (all-oxidized partners) is very much lower than the turnover number obtained under otherwise identical conditions and therefore the measured rate does not apply to the physiologically relevant collisional complex between the two partners in different oxidation states (and not both oxidized as in the electrostatic equilibrium complex). This is also supported by the observation that eT efficiency within the collisional complex is higher and not lower at ionic strengths (0.11 M) at which the electrostatic complex is considerably weakened. (ii) In the burst phase of the reaction with ferrocytochrome c, two electrons are delivered to the oxidase; if product dissociation were rate-limiting this result would be difficult to account unless with

Scheme 4. (iii) Below a certain threshold concentration (estimate: 5 μM, see Bickar et al. [165] for discussion and below), it is expected that O_2 would limit the eT processes in COX: again if the ferricytochrome *c* dissociation limited the measured rate, it would be very difficult to give a physical explanation on how O_2 binding would bring about an increase in the dissociation efficiency of product, also considering that in pulsed and resting oxidases the on-rates of cytochrome *c* binding and oxidation are, within the error, very similar yet the catalytic efficiencies quite different.

If product dissociation is not rate-limiting, then a one-electron intersite eT must be the rate-limiting step. Substantial evidence has been produced to show that is the eT process between cytochrome a–Cu_A and the binuclear site (Cu_B?) (see [1] for review). At this point it must be stressed that considerable confusion has arisen when describing this process. The catalytic cycle of COX is definitely split into two functionally competent parts (see Fig. 10); whether the two reflect actual conformations is difficult to establish at present, but the following discussion applies also. In the absence of O_2, eT to the binuclear site is quite slow, while in its presence, a dramatic increase in the rate constants is observed. These differences depend on the chemical structure of the binuclear center. When cytochrome a_3–Cu_B is oxidised, reduction is slow, while when the site has received 2/3 electrons and has transferred them to bound O_2, it will be fast (as demonstrated by the flow–flash experiments described in the following sections). Consistent with the Marcus theory the coordination of the metals in the binuclear center (which accepts electrons during the reaction) is one of the parameters affecting the eT kinetics via the reorganizational energy term. The experiments of Woodruff et al. [168] indicate that in resting COX an endogenous ligand may be coordinated to the distal side of cytochrome a_3, and thereby affect the kinetics of reduction of cytochrome a_3 by a thermodynamic control (ferric cytochrome a_3 ligands usually tend to decrease the standard redox potential of the site) and/or the bimolecular reaction with exogenous ligands (such as cyanide and azide, but also O_2 and possibly CO). We shall now present in some detail experimental data on reduction and reoxidation of the binuclear center.

2.5. Internal eT to the oxidized binuclear center

In view of the high reactivity of reduced COX for O_2 (see below), the kinetics of reduction of the binuclear center must be investigated under strict anaerobiosis. Under these conditions, it was shown long ago that the rate of appearance of the CO-binding capacity in the resting enzyme was so slow as to be incompatible with the turnover number of the enzyme (50–100 s^{-1}); a two-state model of COX [88,101] has offered a possible explanation for the observed discrepancy. Resting COX is kinetically sluggish; by reduction of this enzyme state and exposure to O_2, however, it is possible to generate pulsed COX, in which the turnover number is considerably (ca. 10-fold) increased. The differences between resting and pulsed (see Section 2.2) COX are likely to be correlated with the chemical structure of the binuclear site, and, indeed, an atypical EPR signal (the '$g = 5$' signal) has been detected following exposure of reduced COX to dioxygen [86,87,89]; this signal decays as pulsed COX decays to resting. It is therefore very likely that pulsed COX may represent the 'only' state of the enzyme present in native membranes.

In view of what outlined above, it is sensible to measure the rate of reduction of oxidized cytochrome a_3–Cu_B site in the absence of O_2 starting from pulsed COX; if so it is useful to take into account four parameters, i.e. (1) generation of pulsed COX and its concentration; (2) the O_2 concentration necessary and sufficient to produce pulsed COX; (3) the type and concentration of reductant and (4) a trapping ligand with high affinity for ferrous cytochrome a_3 (i.e. CO). A protocol for the determination of the rate of cytochrome a_3 reduction takes these factors into consideration [169,170], and a typical experiment is shown in Fig. 11a. Using this experimental design and carrying out experiments at different CO, cytochrome c^{2+} and COX concentrations it was shown that the eT process to the binuclear center is monomolecular, and it involves two discrete eT events, at variance with what has been usually thought [171]. The first reduces presumably Cu_B, while the second slower process reduces cytochrome a_3, leading to complete reduction of the binuclear site and binding of CO (the trapping ligand). The unmentioned eT processes appear to be pH

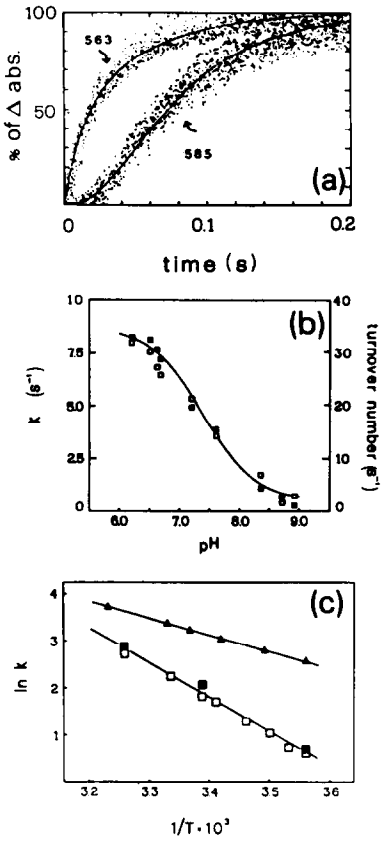

Fig. 11. (a) Internal eT to the binuclear center in beef heart COX. The protein (20 μM), initially reduced and in the presence of excess cytochrome *c* (100 μM) is mixed in the stopped-flow apparatus with a solution containing O_2 stoichiometric with respect to the protein and 1 mM carbon monoxide. In the dead-time of the stopped-flow apparatus, fully reduced COX is completely oxidized and partially rereduced (with electrons residing on the cytochrome a–Cu_A sites). The subsequent events, which are observed, indicate that reduction of the binuclear site occurs prior to CO binding (the 563 and 585 nm traces represent cytochrome *c* oxidation and CO compound formation, respectively). $T = 34.5$°C. (b) pH and (c) temperature dependence of the internal eT processes. In (b) compare left and right ordinates which represent the internal eT rates determined according to this protocol and the turnover number of COX measured independently on the same material. Notice the factor of 4 of the scales to account for the stoichiometry of the COX reaction [see Eq. (1)]. In (c) the upper line reports the temperature dependence of CO binding determined separately. Reproduced from [170] with permission. See [106,169,170] for experimental details.

dependent, the rates diverging at acidic pH values. When the experiment is carried out in the presence of excess O_2, the turnover number of the enzyme in detergent displays the same pH and temperature dependence ($pK_a = 7.4$ and $E_a = 14.7$ kcal/mol) as the internal eT rate (multiplied by 4) under wide conditions of pH, temperature and detergent type (see Fig. 11b and c); this conclusion has been extended to the reconstituted state [106]. Moreover, the turnover numbers obtained in these experiments are quite similar to those obtained previously in steady-state measurements [172,173]. The consequences of these findings are: (i) CO (and presumably O_2) will not bind to the binuclear site until two electrons reside therein; (ii) electrons are not transferred in pairs, but singularly and (iii) the eT processes to the oxidized binuclear site limits the rate and accounts for the turnover number. These findings support the view (already discussed above) that the rate limiting step in catalysis is the internal eT to the oxidised binuclear center.

Any analysis of the eT processes in COX must take into account some experimental findings: (i) the internal eT kinetics are slow when starting from oxidized COX as described above; (ii) in some states of the protein, i.e. photolyzed CO–mixed valence COX, the observed processes are very fast; (iii) the eT events are O_2-dependent and saturation is observed at about 5 μM O_2 [165] and (iv) eT to the 'activated' binuclear center, which carries partially reduced oxygen intermediates (see right part of Fig. 10), is fast. Consequence of this complex experimental scenario is that there is considerable confusion in the literature concerning the magnitude of the eT rates to the oxidized binuclear center. Essentially two experimental approaches are followed. The *first* begins with the reduction of oxidized or pulsed COX (as described above [169,170]); the *second* starts from the (fully or partially) reduced COX in combination with CO and the eT events are studied following the photolytic removal of the ligand and combination of O_2 [154,166,167]; as described in the next section, very fast kinetic processes take place since O_2 greatly enhances the exoergonicity of the reaction. Therefore the CO–mixed valence derivative of COX has been extensively used to probe the kinetics of internal eT in the absence of O_2. In brief, a sample of CO–mixed valence COX is photolysed by a laser pulse to generate an enzyme species which is formally equivalent to species 11 in Fig. 10 (but see below). If this species is thermodynamically unsta-

ble, reverse eT processes take place with partial and transient reduction of cytochrome *a* and Cu_A [153,154,166]. These processes may proceed significantly if they are faster than CO rebinding (k_{on} for CO is 5×10^4 M^{-1} s^{-1}) which occurs on a time scale of tenths of milliseconds (at [CO] = 1 mM). An electron backflow to the cytochrome a–Cu_A sites is observed, with a time course usually biphasic (relaxation rates 10^5 and 10^4 s^{-1}, respectively) and with cytochrome *a* being reduced first. Thus, internal eT is apparently very fast and in severe contrast to the corresponding experiments carried out starting with oxidized COX. This discrepancy may be solved if it is assumed that the structure and coordination of the binuclear site is dramatically different in the two types of protocols. The difference in the two states may very likely involve: (i) the presence of an endogenous (shuttling) ligand with differential affinity to either of the latter metals depending on their redox state and/or presence of gaseous ligand (CO or O_2) [168]; (ii) binding of CO to Cu_B following the primary photolytic event [174]; or (iii) the conformational state of the binuclear site in the photolysed CO–mixed valence intermediate being different from that of oxidised COX. Scheme 2 depicts a simple mechanism which accounts for these considerations. In this scheme only the cytochrome a_3–Cu_B metals are shown in their oxidized and reduced states and in two conformations as indicated by the deponents A and B. Horizontal transitions indicate eT from the cytochrome a–Cu_A sites (shown as 2-eT processes for simplicity) or ligand (X = CO or O_2) binding; vertical transitions represent conformational equilibria (in the oxidized O_{AB} and reduced R_{AB} states). If the conformational equilibria are slow compared to eT_B (where the eT efficiency is such that $eT_B \gg eT_A$) and if only conformation B is efficient in ligand binding, then the kinetics of eT will depend on initial state (conformation) of the enzyme and on whether O_2 or CO are present. Starting from the oxidized enzyme (the $[Fe^{3+}\ Cu^{2+}]_A$ state) and in the absence of ligands the observed eT processes will be slow (eT_A); on the other hand following the photolytic removal of CO from mixed valence COX, the $[Fe^{2+}\ Cu^{1+}]_B$ species will be generated and the subsequent kinetic processes will be fast (eT_B). This mechanism to some extent is also capable of explaining the apparent O_2 and/or CO concentration dependencies of the internal eT processes [165]. In the absence of gaseous ligands, the position of the equilibrium will depend on the exogenous reductant concentration and the time needed to reach the equilibrium on the value of the rate constant of the slowest process (either eT_A or the conformational equilibria $O_{AB} \rightleftharpoons R_{AB}$). When O_2 or CO are present, however, the system is in disequilibrium, especially with dioxygen and at steady-state, and the slowest process may be kinetically shunted. The presence of two conformations with different thermodynamic and kinetic properties is expected if COX is to operate as redox-linked proton pump (alternating access of the proton from topologically distinct aqueous phases) [97,157]. As discussed above, the differences in eT efficiency of the two putative conformations may be attributed to structural transitions of the cytochrome a_3–Cu_B site whose role is to gate electron flow and couple it to proton translocation. The most efficient way to gating electron flow in COX is to vary the reorganizational energy, as predicted by the Marcus theory [175] and discussed by Gray and Malmström [176], since lowering the latter at constant driving force and intersite distance has the effect of making the structure of the oxidized binuclear site in conformation B very similar to that of the reduced state, with consequent increase in rate.

2.6. Oxygen binding and reduction

Molecular oxygen reacts very rapidly with fully or partially reduced COX [177–183]. This reaction is usually studied by mixing the carbon monoxide

$$\begin{array}{ccc} [Fe^{3+}\ Cu^{2+}]_A & \overset{eT_A}{\rightleftharpoons} & [Fe^{2+}\ Cu^{1+}]_A \\ {\scriptstyle O_{AB}}\downarrow\uparrow & & {\scriptstyle R_{AB}}\downarrow\uparrow \\ [Fe^{3+}\ Cu^{2+}]_B & \overset{eT_B}{\rightleftharpoons} & [Fe^{2+}\ Cu^{1+}]_B \overset{X}{\rightleftharpoons} [Fe^{2+}\ Cu^{1+}]_B \cdot X \end{array}$$

Scheme 2.

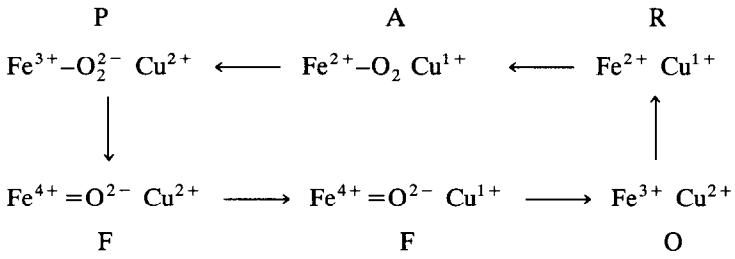

Scheme 3.

derivative of the enzyme (either fully reduced or in the mixed valence state) with oxygen-containing buffer and firing a flash of light. Exposure of reduced COX to O_2 leads to very rapid oxidation of the enzyme. The reaction occurs on a time scale of μs to ms and is too fast to be investigated in a conventional stopped-flow. Therefore, identification of intermediates in this reaction has taken advantage of the properties of the CO complex, which has a very slow thermal dissociation ($k = 0.02$–0.04 s^{-1} [184,1]), but is strongly photosensitive (like all carbonylated heme proteins). Thus, in all cases the relevant overall processes are as follows:

$$a^{2+}a_3^{2+} * CO \xrightarrow{h\upsilon} a^{2+}a_3^{2+} + CO \,(\text{ps to } \mu\text{s})$$

$$a^{2+}a_3^{2+} + O_2\, a^{3+}a_3^{3+} + H_2O \,(\mu\text{s to ms})$$

Fe^{2+}	Cu^+	Reduced (R) or mixed valence (MV)
O_2 ⇓		on: 3×10^8 M^{-1} s^{-1}; off: 2×10^3–4×10^4 s^{-1}
Fe^{2+}	Cu^+-O_2	Primary adduct
↓		3–3.5×10^4 s^{-1}
$Fe^{2+}-O_2$	Cu^+	Compound A, photosensitive
↓		very fast or 4.5×10^3 s^{-1} in MV
$Fe^{3+}-O_2^{2-}$	Cu^{2+}	Primary P = peroxy
↓		2×10^5 s^{-1}, electron from cyt. *a*, H^+ from protein acid–base group
$Fe^{3+}-O_2H^-$	Cu^+	Secondary P species
↓		10^3 s^{-1}, heterolytic O–O breakage
$Fe^{4+}=O^{2-}$	$Cu^{2+}-OH^-$	Primary F = ferryl eT from cyt. *a* at 2×10^5 s^{-1} rate-limited by the Cu_A-to-cyt. *a* eT process, i.e. 6000 s^{-1} or by proton uptake
$Fe^{4+}=O^{2-}$	$Cu^{2+}-OH_2$	Secondary F species
↓		Rate-limited by?
$Fe^{3+}-OH^-$	$Cu^{2+}-OH^-$	Hydroxy species (pulsed?)

Scheme 4.

Optical data [168] have indicated that the rate of the first observable process is oxygen-dependent up to 20–30 000 s^{-1} (with a bimolecular rate constant of 10^8 M^{-1} s^{-1} at 4°C). Two additional processes, with rate constants of ca. 7000 and 5–700 s^{-1}, have been assigned in an early sequential scheme to eT from Cu_A and cytochrome *a*, respectively. However, the mechanism proved to be considerably more complex, and model information on the pathways of eT to oxygen from the binuclear center metal atoms and the other redox sites have been studied by room temperature and cryogenic measurements, by optical, EPR and RR spectroscopy [185–188].

The O_2 reaction will be initially discussed with reference to Scheme 3, which is a simplified version indicating six species of the two metals in the binuclear center (as proposed by Babcock and Wikström [97]).

The nature of the major intermediates in the reaction of O_2 with the binuclear center has been recently elucidated by RR spectroscopy [189–194], a technique that allows, for example, the identification of the iron-ligand stretching modes (and thus capable of proposing structures [195]). A more complete scheme, which is a summary of the information obtained by transient RR and electronic spectroscopy is shown in Scheme 4 [192,193,195]; in the following discussion we shall refer to the simpler or the more complete schemes, according to the data discussed.

Binding of O_2 demands that both metals of the binuclear center are in the lower oxidation state, as found for CO. The *primary intermediate* according to Han et al. [189] is shown to be an oxygen complex of the iron of cytochrome a_3, very similar to oxymyoglobin and oxy-hemoglobin (characterized by an Fe–O_2 stretching mode in the RR spectrum at 568 cm^{-1}), and is likely to have a ferric-superoxide structure. The RR data confirm the proposal of Chance et al. [185,186], that this intermediate, (i.e. compound A) is an oxygen complex with characteristic absorption peaks at 535 and 586 nm and a through at 604 nm. The oxygen affinity has also been estimated [165] $K = 5 \times 10^4$ M^{-1} at 5°C (with $k_{on} = 10^8$ M^{-1} s^{-1} and $k_{off} = 2000$ s^{-1}).

Compound A has the same spectral features when starting with the fully reduced or the mixed valence state of the enzyme. However, its lifetime is considerably different in the two cases: compound A in the mixed valence state is relatively long-lived ($k = 4.5 \times 10^3$ s^{-1}), while it decays more rapidly ($k = 3.5 \times 10^4$ s^{-1}) in the reduced enzyme. In both cases the subsequent eT reaction leads to an intermediate in which dioxygen has received two electrons (and must be a peroxide-like intermediate bound to cytochrome a_3); however, the species resulting from the eT reactions to bound O_2 are different when starting from the mixed valence or the fully reduced enzymes: in the former case all the metal centers are oxidized while in the latter Cu_B is reduced, the second electron being delivered to dioxygen directly from cytochrome *a*. This is a rather unconventional viewpoint since it was usually thought that the decay of the [Fe^{2+}–O_2 Cu^{1+}] species occurs by direct eT within the cytochrome a_3–Cu_B site [196–198].

The chemical structure of the primary intermediate (or compound A) has been recently challenged. Firstly, in a recent room temperature time-resolved infrared study [174] of the super-rapid events occurring after photodissociation of CO from reduced COX, it was conclusively shown that photodissociated CO binds quantitatively to cuprous Cu_B prior to equilibrating with the bulk solution. Secondly, the flow–flash experiments of Blackmore et al. [199] have shown that appearance of a photosensitive species with the spectral properties of compound A (i.e. Fe^{2+}–O_2) is populated with a first-order (not

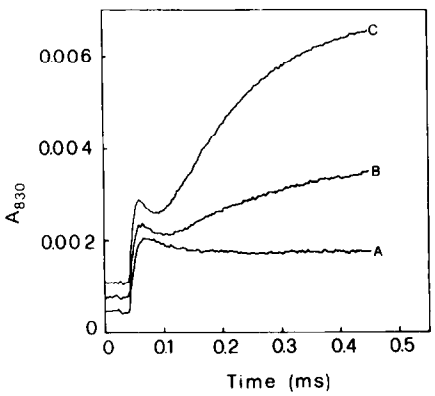

Fig. 12. The O_2 reaction as followed at 830 nm. Flow–flash experiment in the presence of 1 mM O_2 showing the time course of absorbance changes monitored at 830 nm of 4 μM COX in the initially: (A) mixed valence + CO, (B) 3-electron reduced + CO, or (C) fully reduced + CO states. Reproduced with permission from [200].

$$Fe^{2+}\ Cu^{+} \underset{k_{off}}{\overset{k_{on}\cdot O_2}{\rightleftharpoons}} Fe^{2+}\ Cu^{+}\cdot O_2 \xrightarrow{k_t} Fe^{2+}\cdot O_2\ Cu^{+}$$

Scheme 5.

second-order) rate constant of 3.5×10^4 s^{-1} as determined at high O_2, suggesting that O_2, on its way to ferrous cytochrome a_3, binds in a bimolecular mode to reduced Cu_B. Finally the experiments of Oliveberg and Malmström [200] provide direct evidence for binding of dioxygen to Cu_B as probed at 830 nm where the transient Cu_B–O_2 species is proposed to absorb. This experiment is shown in Fig. 12. The initial events for binding of O_2 to the reduced binuclear center are therefore schematically shown in Scheme 5, where $k_{on} = 1 - 3.5 \times 10^8$ M^{-1} s^{-1}, $k_{off} = 2 \times 10^3$ to 5×10^4 s^{-1}, and $k_t = 3 \times 10^4$ s^{-1}.

The species likely to bind O_2 during turnover all share the common feature of having both metals in the binuclear site reduced and are labeled by asterisks in Fig. 10. These are: (i) the fully reduced species, (ii) two 3-electron reduced species or (iii) one 2-electron reduced species (the mixed valence enzyme). Although there is general consensus that all four species are *competent* for O_2 binding, it is not agreed which is the *dominant* species, i.e. the intermediate whose steady-state concentration is highest, or even if different species may be the prevailing O_2-binding states under different conditions (e.g. at different O_2 and cytochrome *c* concentrations). As discussed recently [201], if eT to the oxidized binuclear site is rate-limiting, then under physiological conditions the mixed-valence intermediate should not be significantly populated at steady state and therefore the fully reduced enzyme should take over. However, at high O_2 (> 50 μM) and low cytochrome *c* (< 100 μM), the prevailing O_2-binding species is very likely the mixed-valence form (a^{3+} Cu_A^{2+} a_3^{2+} Cu_B^{1+}) [202,203]. This is an important aspect since the chemical nature of the O_2-binding species may be linked to the efficiency of proton translocation, according to an hypothesis proposed by Babcock and Wikström [97].

Following formation of compound A, rapid eT events take place to reduce bound O_2. Transfer of two electrons yields the peroxy intermediate (P-labeled species Scheme 3 and in Fig. 10). Its rate of formation, as discussed above, depends on the initial degree of reduction of the protein, being slowest in mixed valence COX. This view is not totally agreed as according to Oliveberg and Malmström [200] the rate of formation of P in the reduced and mixed valence states may be identical. A crucial point is to establish the oxidation state of Cu_B in P, which is reduced starting from partially or completely reduced COX. This is intriguing since oxidation of Cu_B in mixed valence is slow (4.5×10^3 s^{-1}) as compared to formation of P in the other enzyme forms ($> 3 \times 10^4$ s^{-1}). These findings may imply that P obtained from mixed valence COX is an artificial species with no physiological counterpart. If Cu_B is reduced in P, then the second electron must come from another metal kinetically more efficient; the most remarkable result of the RR experiments of Han et al. [190] is the suggestion that the metal center involved is cytochrome *a*. However, owing to the very short distance between cytochrome a_3 and Cu_B (5 Å), a very fast concerted two eT process to bound O_2 was expected (the second electron being provided by Cu_B). Therefore, since formation of P (species No. 22 in Fig. 10) is rate-limited by formation of compound A, the actual cytochrome *a* to cupric Cu_B eT process is likely to be much faster, as suggested by Oliveberg and Malmström [200] and others [201] (2×10^5 s^{-1}), with production of P proposed by [190] containing a ferric-peroxide–cuprous binuclear site.

Two further kinetic processes are observed with rate constants of the order of 5–7000 and 500–1000 s^{-1}, respectively. Two intermediates have been well characterized by RR spectroscopy using oxygen-isotope sensitive lines [194,195]. The first intermediate is ferryl–oxo species ($Fe^{4+}=O^{2-}$), denoted by an F in Scheme 3 and Fig. 10, identified by RR line at 786 cm^{-1}, and a 35 cm^{-1} oxygen isotope shift. This intermediate, which is maximally populated within 0.5 ms, is at three-electron reduction level and the oxygen atom is apparently hydrogen-bonded, possibly to a water molecule bound to Cu_B (proposed to be in the higher oxidation state). The formation of F

is associated to heterolytic cleavage of the O–O bond of O_2 in a process which displays the highest temperature dependence and has a rate constant of ca. 1000 s^{-1}, as observed in EPR [75] and flow–flash experiments [196]. Alternatively the eT from Cu_B could be more facile, the actual O–O bond breakage limiting the rate [1].

As F decays, a new intermediate with an RR isotope-sensitive line at 450 cm^{-1} is formed and has been assigned to an Fe^{3+}–OH^{-1} complex of cytochrome a_3 [194]. This species persists up to 3 ms, which means that transfer of the fourth electron to the binuclear site is apparently the slowest eT event [5–700 s^{-1}] in the oxidative reactions of COX [146] (yet still faster than the eT events to the oxidized binuclear site).

In addition, in most of the flow–flash experiments a 5–7000 s^{-1} phase is observed. This corresponds to an absorbance increase both at 445 (the so-called 'bump' phase) and 830 nm and may therefore represent reduction of cytochrome a by Cu_A in those enzyme intermediates in which the binuclear site is at the peroxide level with Cu_B reduced. This interpretation is also consistent with the reverse eT experiments following removal of CO in the absence of O_2 at various degrees of reduction of mixed valence COX (see above and Scheme 4).

The P and F species can also be generated chemically [141,162]. The former can be prepared by reaction of the carbon monoxide mixed valence derivative with O_2, and has a life-time of ca. 20 minutes. The latter is generated [204] by treatment of the oxidized enzyme with an excess of hydrogen peroxide (10 mM). In both cases, however, it is not clear whether these two species are true representations of the corresponding intermediates obtained during (one) turnover flow–flash experiments.

These investigations establish that there are independent eT pathways within the enzyme. Thus, electrons may be delivered (albeit at different rates) independently from cytochrome a or Cu_A to the binuclear site, and depending on the redox state of Cu_B directly to cytochrome a_3. Parallel eT pathways may not be fortuitous since in vivo these may be linked to special functions, such as proton translocation and control of energy transduction [205]. Moreover, two notable cases, the photosynthetic reaction center protein [207] and the multicopper protein ascorbate oxidase [208], show split eT pathways in the protein matrix, though the precise significance for the observed eT pathway selectivity has not been put forward.

From the discussions in this section it is shown that the eT processes to the O_2-activated binuclear site are very complex [206]. It also appears that the kinetic efficiency is apparently damped progressively as the intermediates are populated. Moreover, it is evident that every single eT process (with the exception of formation of P which has the properties of a 2 eT process) is quite different from each other. This may be possibly explained by considering that the target of eT to the activated binuclear is quite different in each intermediate, and therefore that the parameters governing eT will be different and affect the rate, according to Marcus theory [175].

3. Energy transduction and vectorial processes

3.1. Electron transfer and proton translocation

Cytochrome oxidases display a further important function, i.e. the coupling of the eT reactions to vectorial transport of protons from the matrix aqueous space to the intermembrane space of mitochondria. In aerobic prokaryotes, this corresponds to proton translocation from the cytoplasm to the periplasmic space (in contact with the outside world). This function contributes to the generation of a proton electrochemical gradient which is used by the cell in a variety of metabolic processes such as ATP synthesis and ion and metabolite transport. Proton pumping by COX occurs according to reaction (5):

$$4c^{2+} + (4+n)H_m^+ + O_2 \rightarrow 4c^{3+} + nH_c^+ + 2H_2O \quad (5)$$

[1] F displays an unusual reactivity towards CO (which is still present in the solution during these experiments) and as a result an oxo-transfer reaction takes place from F to CO to yield CO_2 with concomitant reduction of cytochrome a_3 to the ferrous state [203]. If in this intermediate Cu_B is oxidized then it should be detectable by EPR, as observed (see Fig. 6). However, the rate of the reaction displays a half-time of 4 minutes a 277 K which excludes any interference with all the above eT processes.

where the subscripts m and c indicate the matrix and cytoplasmic sides of the mitochondrial membrane, respectively, and n represents the number of H^+ translocated by COX per electron transferred to O_2. The proton pumping function of COX, as represented in Eq. (5) has been demonstrated by Wikström et al. in 1977 [4], though, up-to-date, there is no general consensus on the exact value of n, since the mechanism of proton pumping has not been unraveled. It is not established, for example, if the value of n is fixed or variable, which in turn may be linked to a direct or an indirect proton–electron coupling mechanism. The value of n, i.e. the number of protons that are vectorially translocated across the membrane, has been reported to vary between 2 and 8, yielding a H^+/e^- ratio of 0.5 to 2, though, at present it is generally agreed that the phenomenological stoichiometry approaches unity. Since proton translocation was discovered in respiring mitochondria [4], many investigations have been carried out both in mitochondria and in artificial vesicular systems containing COX, the results supporting the initial proposal [209–213].

The properties of COX reconstituted into unilamellar vesicles obtained according to the cholate dialysis method [210,214–217] have been systematically studied (see Table 3). According to this technique detergent-solubilized COX is added to a presonicated mixture of phospholipids (i.e. asolectin, lipids from soybean) and a dialysible detergent, such as sodium cholate. Slow detergent removal results in the incorporation ('reconstitution') of COX into the artificial phospholipid bilayer to yield the COV preparation (cytochrome oxidase reconstituted into vesicles). These preparations have been extensively characterized (see Table 3 for a synopsis of molecular properties) in terms of lipid composition [218], dimensions [219,220], sidedness of COX with respect to the membrane [214,217], the aggregation state of COX in the membrane [18,221], buffer power [222] (which is a conditio sine qua non for the correct estimate of the redox-linked protonic events, and is unfortunately misregarded in the literature), steady-state [223–231] and transient kinetic properties [106,232], proton translocation and respiratory control (RCR) [4,17,212–214,229,230].

COX is a molecular machine since part of the redox free energy is transduced into a proton electrochemical gradient ($\Delta\tilde{\mu}_{H^+}$). There are two reactions by which COX contributes to the development and maintenance of $\Delta\tilde{\mu}_{H^+}$. First of all, since the reductant of COX, namely ferrocytochrome c, reacts with the protein on the cytoplasmic side of the mitochondrial membrane, the transmembrane charge transfer leading to formation of H_2O provides a physical mechanism for the capacitative charging of the bilayer because protons are consumed from the matrix [233]; thus transmembrane eT is associated per se to the development of a membrane potential. If O_2 reduction occurs in a space in protonic contact with

Table 3
Properties of vesicular cytochrome oxidase (COV)

		Ref.
Phospholipid [a] composition % (w/w)	PE: 37, PC: 36, DPG: 9, others: 18	[218]
Liposome dimensions (diameters)	14 to 37 nm [b]	[219,220]
COX particles pervesicle [c]	1 (58), 2 (26), 3 (11), 4 (5)	[219]
Sideness	80–90% mithochondrial-like	[214,217]
Aggregation state of COX	dimer or functionally interacting monomers or monomers	[18,221]
Buffer power	outer leaflet: 0.26 mM · pH^{-1}	[222]
	inner leaflet: 0.22 mM · pH^{-1}	[222]
RCR	4–20	[214–217,229]
Observed H^+/e^-	1	[17,230]
Sensitivity [d]	C: poor, C + V: high, N: none,	see text and [226,232]
to ionophores	N + V: high, V: high but time dependent	

[a] PE = Phosphatidylethanolamine; PC = phosphatidylcholine; DPG = diphosphatidylglycerol.
[b] The average diameters may be decreased by reconstitution in the presence of polyvinylalkanoate polymers, see [207].
[c] Numbers in parenthesis indicate the percentage of vesicles having particles.
[d] C = Carbonylcyanide-*m*-chlorophenylhydrazone; N = nigericin; V = valinomycin.

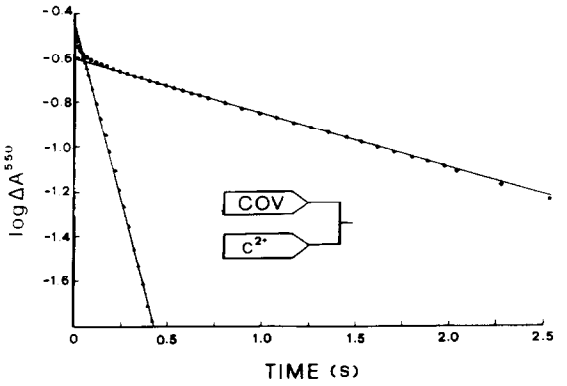

Fig. 13. Kinetics of cytochrome *c* oxidation by COV. 1.25 μM COV are mixed in the stopped-flow apparatus against 20 μM ferrocytochrome *c*. Suspending medium: 0.1 M Hepes buffer pH 7.3. Upper trace: the COV syringe contains either no ionophore or 5 μM nigericin; lower trace: the COV syringe contains 10 μM valinomycin plus 10 μM carbonylcyanide-*m*-chlorophenylhydrazone. T = 20°C. RCR = 9.7. See text for details and [232].

the mitochondrial matrix (or vesicle lumen), a transmembrane pH difference will also be produced, the inner space becoming more alkaline; with COV the transmembrane pH difference would eventually vanish, because of back leak. Second, COX is a site for energy transduction, because it mediates the redox-linked vectorial transport of protons in a direction *opposite* to the eT processes, this is the proton pumping function of oxidases. This process is clearly electrogenic as the charge must be translocated across the membrane dielectric and at equilibrium an equivalent amount must be back-transported to achieve chemical and electrical neutrality, as demonstrated by the counter-fluxes of Ca^{2+} or K^+ ions [212,234].

The kinetics of cytochrome *c* oxidation by COV have been extensively studied by stopped-flow spectroscopy [106,225,226,232]. When COV are mixed with ferrocytochrome *c*, in the presence of excess O_2, biphasic kinetics [232] are observed at wavelengths monitoring the redox state of cytochrome *c* (Fig. 13). At this wavelength, the fast phase (whose amplitude depends on the ratio of cytochrome *c* to COV) accounts for the oxidation of (at least) four moles of ferrocytochrome *c* per mole of COX. The subsequent slower phase is essentially exponential for the rest of the time course, and its first-order rate constant reflects a property of the enzyme that is populated during turnover. The respiratory control (RCR) [214] is defined operationally as the ratio of steady-state oxidation rates of ferrocytochrome *c* in the presence of ionophores (such as nigericin or carbonylcyanide–*m*-chlorophenylhydrazone plus valinomycin) to that in their absence, i.e. the ratio of rates observed under conditions in which the membrane is totally leaky to ions relative to the situation in which the intrinsic ion permeability of the membrane is the eT-limiting factor, in the classical sense. The RCR, as measured by the ratio of the rate constants of the fast to the slow phases of cytochrome *c* oxidation in the absence of ionophores (in Fig. 13), closely approximates the RCR measured in two independent experiments following the oxidation of cytochrome c^{2+} in the presence and absence of ionophores (the time course being in both cases an exponential process in the turnover phase).

The classical interpretation of this observation is that catalysis is rate-limited by the protonic back-leak rate inside the vesicle lumen which is quite slow even in the presence of a fully developed $\Delta\tilde{\mu}_{H^+}$ (ca. 0.15 s^{-1} and much lower, 0.02–0.04 s^{-1}, in the presence of valinomycin, as measured by use of a membrane impermeable pH indicator [232]). However the protonic back-leak rate is slower than cytochrome *c* oxidation in fully coupled COV. This may be consistent with the higher efficiency of the proton in dissipating $\Delta\tilde{\mu}_{H^+}$ relative to other ions in the steady-state regime, since proton transport inside the vesicles collapses simultaneously both components of $\Delta\tilde{\mu}_{H^+}$. Moreover, cytochrome *c* oxidation is largely insensitive to the effect of nigericin, which exchanges protons for potassium ions electroneutrally, and consistently enhances the protonic transmembrane transfer. Under these conditions: (i) the driving force is not changed, (ii) the chemical component of $\Delta\tilde{\mu}_{H^+}$, i.e. ΔpH, is abolished, (iii) $\Delta\psi$ must increase to match the driving force (yet without effect on the eT efficiency, an indication that after completion of 1–2 enzyme turnovers static head is already reached), and (iv) proton movements are apparently not related to the catalytic efficiency of COV. Finally, in going from resting to pulsed [88] COV, the rate of cytochrome *c* oxidation increases by the same factor both in the presence and absence of ionophores (i.e. the RCR is identical) [107] a fact which may be difficult to explain if the turnover rate in the absence of ionophores were limited by proton back diffusion through the membrane.

If the ΔpH is not influent as far as eT is concerned (the effect being limited to the first few turnovers [226]), the electrical component must exert its influence on the observed eT kinetics. As a matter of fact the electrogenic uniporter valinomycin greatly increases the rate of oxidation of ferrocytochrome *c*, approaching more than 80% of the observed RCR. The lack of a complete effect may be due to chemical effects related to the number of protons in the interior space [226] which, in the vesicles is quite small (volume = ca. 4×10^{-21} l, based on vesicle diameter of 30 nm and a membrane thickness of 5 nm; in an unbuffered medium at pH = 3 this would correspond to about 140,000 water molecules and 3 protons!); therefore: (i) the absolute amount of protons becomes limiting, also in a well buffered preparation, when many enzyme turnovers have been completed and/or (ii) if the bilayer concentration of valinomycin is small, the ionophore may not be homogeneously partitioned between all the vesicles or its concentration may even be higher in the aqueous bulk phase; therefore its membrane potential quenching activity may become less efficient.

The observed kinetics of eT in COV appear to underlie a saturation phenomenon [232,235], the enzyme responding to the build-up of the gradient in a fashion similar to ligand binding, where the 'ligand' is represented by $\Delta\psi$. This interpretation is also consistent with the predicted and observed increase of the RCR, at constant driving force, as the vesicle dimension is artificially decreased by incorporation into the bilayer of synthetic polyvinylalkanoates [220]. Treatment of COV as spherical capacitors also reproduces their kinetic properties [205].

Experimental evidence for the proton pumping activity of COV has been obtained by two different techniques (see [217] for the relevant methodology): (a) potentiometric and (b) spectroscopic. Several groups have successfully employed pH indicators (e.g. phenol or neutral red) to measure redox-linked acidification of the bulk during turnover. These have the great advantage of a rapid response and have proved uniquely valuable in measuring pH changes. The drawbacks are that often artifacts are produced and should be accounted for. The use of a glass electrode, besides the obvious advantage of a direct measurement of the proton activity, is bound to have some shortcomings, apart from the obvious fact that pH measurements are possible only in the bulk. The intrinsically slow response of the glass electrode may pose some problems of reliability of quantitative estimates, especially for COV preparations which display a high proton leak rate (i.e. low RCR). Rapid-mixing techniques are, in this respect, clearly superior since both early events (proton pumping) are readily resolved from late events (leak).

The kinetics of proton pumping by COV have been studied by sophisticated stopped-flow spectroscopy in our laboratory [213]. The time course of proton extrusion into an aqueous bulk phase with no buffer power other than that of the outer leaflet of the phospholipid bilayer (see Table 3) has been monitored by the changes in extinction of a suitable pH indicator (phenol red, $pK_a = 7.6$) and compared to the time course of oxidation of ferrocytochrome *c*. It must be recalled that the outer leaflet buffer power is only transiently effective since at equilibrium and due to the formation of $\Delta\tilde{\mu}_{H^+}$, also the inner leaflet buffer power will come into play; thus the vectorial and scalar H^+/e^- stoichiometries are expected to yield different pH-indicator-linked absorbance amplitudes (larger in the former case [222]). The results indicate that the vectorial and redox processes are synchronous events up to a rate constant of 10 s^{-1}, provided that an efficient charge-compensating system (valinomycin and K^+) is present. More recently [230], these experiments have been repeated by taking advantage of time-resolved photodiode array spectroscopy used in conjunction with singular value decomposition, which decomposes the absorbance–wavelength–time data matrix into the product of three matrices $U \times S \times V^T$ (see Henry and Hofrichter [236] for details) and allows to: (i) remove random noise from the data resulting in a significant increase in the signal-to-noise ratio, (ii) to reduce the enormous amount of data which is acquired (typically spectra of 1024 wavelengths collected at 62 different time points) from 10 ms on and, iii) under specific conditions, to perform efficient chromophoric separation in the wavelength and time domains, a necessity if quantitative evaluation of the apparent H^+/e^- stoichiometry is desired. Fig. 14 shows one such experiment in which the redox-linked vectorial events are followed by time-resolved stopped-flow spectroscopy. The best estimate of the H^+/e^- ratio from these stopped-flow experiments (1.01 ± 0.10) con-

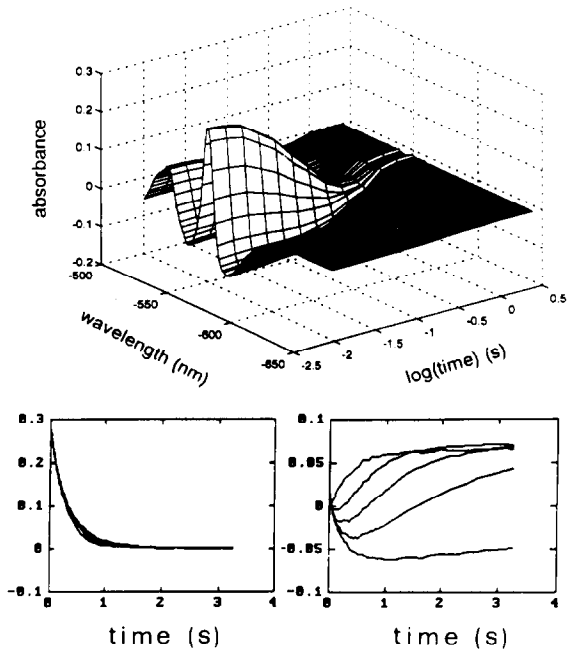

Fig. 14. Kinetics of proton pumping by COV. Upper: 62 time-resolved spectra obtained following mixing COV (1.25 μM) containing valinomycin (10 μM) and carbonylcyanide-*m*-chlorophenylhydrazone (0.1 μM) with phenol red (60 μM) and ferrocytochrome *c* (20 μM). Buffer internal to COV was 0.1 M Hepes pH 7.3; external buffer, 50 μM Hepes/43.6 mM KCl/46.1 mM sucrose, pH 7.3. $T = 20$°C. Lower: time course of cytochrome *c* oxidation (left panel, 550 nm) and proton pumping (right panel, 556.6 nm; downward deflection representing acidification of the external medium) by COV containing 5 μM valinomycin and 0, 0.05, 0.15, 0.35 and 1.25 μM carbonylcyanide-*m*-chlorophenylhydrazone (after mixing), after SVD analysis and spectral reconstruction of the data shown in the upper part. Other conditions as above. See [230] for the complete SVD analysis and for details. Modified from [230] with permission.

firms the findings of other investigators obtained using glass electrode potentiometry.

3.2. Models of proton pumping

In order to achieve proton translocation in COV (as in any redox-linked proton pump), at least two enzyme conformations must exist. See Wyman [237] for a description of the general and relevant principles of linked functions. In the first conformation the access of the proton on the protein must be on one side of the membrane (the M side), while in the second it must be on the opposite side. By the principle of microscopic reversibility it follows, unless otherwise proved, that each conformation is completely competent in the eT reactions which take the electrons from cytochrome *c* to O_2. If each redox cycle were to be completed without any net vectorially-linked conformational transition, then the protons bound at the relevant site(s) at certain stages of the turnover would dissociate into the *same* aqueous bulk phase from which they came from. Thus, no matter which conformation is populated, proton pumping will fail. Each thermodynamically and kinetically 'isolated' conformation would represent, by definition, a slipping state, i.e. a condition which determines decoupling of the driving reaction (eT) from the driven reaction (proton translocation). It follows that in order to couple the two reactions there must be a transition between the two conformational states allowing for protonic binding/debinding in two topologically distinct bulk phases; in other words the vectorial event is made possible by a periodic transition between two redox competent slipping states. This type of coupling is referred to as 'parallel' coupling as opposed to 'sequential' coupling, described below. A classical example of parallel coupling is provided by trout hemoglobin [238] which is capable of effectively 'pumping' O_2 against its concentration gradient in the swim bladder of several fishes. This important function is achieved by the relaxed-tense (R/T) conformational transition of hemoglobin, e.g. essentially a decrease in the O_2 affinity, which is *triggered by* and *linked to* the protonic activity in two separate compartments of the fish.

In the case of 'sequential' coupling the redox-linked vectorial events are always coupled to a conformational transition between input (proton binding from one aqueous domain) and output (proton release from the trans side of the membrane) states. However, the transition is by all purposes part of the catalytic mechanism, and there is no way to decouple the redox reaction from the H^+ transport process, since the conformational change from input to output state is an obligatory step in the overall reaction coordinate pathway.

It is not a simple matter to discriminate between the two extreme types of coupling pertinent to case of COV. In the sequential type of coupling, a fixed (direct) mechanistic H^+/e^- ratio is expected; in

parallel (indirect) coupling both fixed and variable H^+/e^- stoichiometries are possible, depending on the effect of parameters (such as the membrane potential and/or the transmembrane pH difference on the steady-state population of enzyme intermediates) which take to a decoupling or a pumping pathway. Discrimination between these types of schemes must clearly await for further experimentation. For additional details on the mechanisms of proton translocation see the review of Chan and Li [198].

As discussed in Sections 2.3–2.6, the first part of the catalytic cycle of COX (reductive eT to the oxidized binuclear site) is dramatically different from the second (eT processes to bound O_2; compare the time scales of Figs. 11 and 12). If the cytochrome a–a_3 intersite distance is not changed, then a structural rearrangement at the level of the binuclear site is consistent with the increase in eT rate by more than 3 orders of magnitude (10^2 vs. 10^5 s^{-1}, respectively). Wikström [197] has shown by reverse eT experiments in mitochondria that of the four electron transfer steps to the binuclear site only the last two, i.e eT to the P and F species, are linked to the proton translocation events, each vectorial event being effectively a 2 H^+/e^- process. This experiment predicts that proton translocation will lag behind the eT processes to the oxidized binuclear site since the latter occurs only in the second half of the COX reaction (see right part of Fig. 10). On the other hand eT to the oxidized binuclear site (left hand of Fig. 10) in the absence of O_2 is quite slow. This may be well suited for the activity of COX since the eT processes may be limited by a conformational transition, preceded by or coupled to fast proton binding processes, which shuttle the bound protons between different sides of the membrane. The function of O_2 would be then to bind and drive the otherwise unfavourable equilibrium (see Scheme 2) in the translocation direction by virtue of the essentially irreversible O_2-reductive reactions (see Scheme 3). A schematic model proposing a mechanism of coupling between eT and vectorial proton uptake and release is reported in Fig. 15.

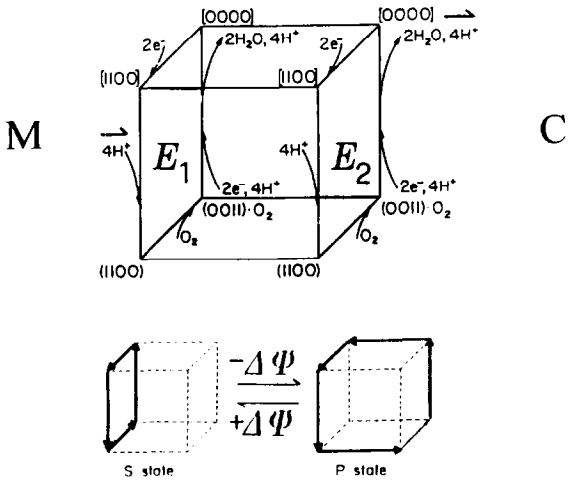

Fig. 15. Coupling of electron transfer and vectorial proton translocation as described by a cubic model. The two lateral faces E_1 and E_2 correspond to two different conformational states of cytochrome oxidase. The digits in parentheses designate the four redox centres in the order (from left to right): cytochrome a, Cu_A, Cu_B and cytochrome a_3, 0 representing an oxidized metal and 1 a reduced one. E_1 and E_2 are supposed to be fully competent in electron transfer, as represented schematically along the four edges limiting the lateral faces E_1 and E_2. The square brackets present in the upper part of the cube indicate the deprotonated state, while the round brackets in the lower part of the cube indicate a protonated state of the enzyme. Vectorial protons are indicated by an arrow. In the bottom part of the figure the bold arrows along the edges of the cubes indicate the prevailing pathway covered by the enzyme in the presence (S state) or absence (P state) of $\Delta\tilde{\mu}_{H^+}$.

3.3. Structural components of the pump

Despite intensive research and efforts, the mechanism of proton pumping, the metal center(s) and subunits directly or indirectly involved are still unknown. It is clear, however, that a metal site must be involved in the vectorial processes since these are intimately linked to the redox activity of COX. It is also apparent that since the metals are all bound to subunits I (cytochrome a, a_3 and Cu_B) and II (Cu_A) (see Section 1.7), these polypeptides, must provide to some extent the molecular architecture allowing for the transport of the proton across the bilayer via membrane-spanning hydrogen-bonded chains of aminoacids [239], in correct orientation, appropriate environment and of proper chemical nature. The site-directed mutagenesis experiments of the Ferguson-Miller and Gennis groups [99,100], which are still under way may provide information concerning the three-dimensional modelling of subunit I (see

Fig. 7), and the role of other conserved residues not involved in metal coordination but essential to the vectorial protonic events.

At different times, all four metal centers have been proposed as structural elements of the pump, i.e. the metal whose redox cycling is coupled to the vectorial proton transport. Cytochrome *a* has been proposed on the basis of strengthening of hydrogen bond between the formyl group of heme *a* and an hitherto undefined protein residue, upon reduction of the enzyme. This experiment [240], which was unique in so far as it proposed a physical mechanism for proton pumping, could not be followed up and substantiated by conclusive data. Cu_A has also been proposed, based on chemical modification of the latter site with mercurials (see Sections 1.4 and 2.3) which resulted in attenuation of the redox-linked acidification amplitude [241]. From these experiments it was also possible to propose a putative mechanism for proton pumping based on a ligand substitution reaction (a cysteine–tyrosine exchange) in the coordination sphere of Cu_A, triggered by reduction of the metal and linked to net proton transport [242]. The role of Cu_A in energy transduction has become less leading, since the superfamily of oxidases contains enzymes which are naturally devoid of Cu_A yet display the proton pumping function (i.e the quinol oxidases).

An important aspect of the coupling of eT to proton translocation in COX is negative redox cooperativity, which is very much pronounced between cytochrome *a* and cytochrome a_3–Cu_B [3]. The redox metal involved is Cu_B and control is exerted thermodynamically: reduction of Cu_B by intramolecular eT processes disfavours reduction of cytochrome *a* and vice versa. According to Babcock and Wikström [97], the special function assigned to the negative redox cooperativity in COX is to prevent electron slip, i.e. movement of electrons without the associated transport of the protons. This situation may arise in the flow–flash experiments using fully reduced COV. Namely, if re-reduction of Cu_B by cytochrome *a* occurs on a time scale faster than the input–output transition of the former metal, then proton pumping will be effectively decoupled from eT (recall that in some states oxidation of cytochrome *a* may proceed as fast as 10^5 s^{-1}, see Section 2.6). This may explain why lower H^+/e^- ratios have been determined by flow-flash starting from the fully reduced CO enzyme [192], which has been proposed to be an 'artificial' species [97]. On the other hand if reduction of cytochrome *a* is prevented in the enzyme states which carry a cuprous Cu_B then the vectorial events may take place without the short-circuiting reactions described above. This proposal, which is essentially based on the neoclassical scheme for redox interactions in COX fails to explain the known steady-state behavior of COV and predicts that the dominant and relevant O_2-binding species during turnover will be the mixed valence enzyme; a matter still controversial [201]; see also [243] for a very stimulating discussion.

It may be worthwhile discussing, as a final remark, some possible functional consequences of the structural model of subunit I proposed by the groups of Gennis and Ferguson-Miller [99,100] (see Section 1.7 and Fig. 7). The bulk of evidence suggests that cytochrome *a* and a_3 are bound to opposite sides of the same helix (X) via His coordination, with a single intervening (totally conserved) Phe residue. Therefore, if correct, the iron of the two hemes *a* and a_3 are connected by 16 covalent bonds, which may provide a pathway for eT. The group of Woodruff and co-workers has proposed a very interesting model based on time-resolved RR and FT-IR experiments [109,244]. According to this model, the binuclear site is labile in the coordination sphere of Cu_B and cytochrome a_3 as a consequence of exogenous ligand entry and binding (including possibly O_2). Binding of CO to Cu_B, for example, causes the release of a ligand from this metal and coordination of CO to the distal side of reduced cytochrome a_3. Displacement of His (419) on helix X (see Fig. 6), documented in some transient intermediates [109], introduces a gap between cytochrome *a* and a_3, which is calculated to dramatically affect the eT rate between the two metals (e.g. by 3 orders of magnitude), without a significant change in the donor–acceptor distance. eT rates are dramatically different when the binuclear site is oxidised relative to that observed in the P and F states of COX (see Sections 2.5 and 2.6). This large difference may be explained by an increase in the driving force term due to O_2 binding, but also by 'reorganization' of the electron transfer pathway connecting the relevant metal centers [175,245]; the latter hypothesis is (in our view)

[246] more likely because in photolysed mixed-valence COX (where CO has escaped to the bulk) there is no exogenous ligand bound to the binuclear site, yet eT is fast [153,154,166]. This opens a new way of looking at the problem of modulation of eT in COX via changes in the coordination sphere of cytochrome a_3, which may represent a molecular mechanism for control of eT rates and coupling of eT to H^+ pumping. Some elaborate, yet stimulating, hypotheses for the involvement of the ligand-switch in H^+ pumping have in fact been recently proposed by Rousseau et al. [247] and Woodruff [109], and represent a challenge for new experiments on the mechanism of H^+ pumping by terminal oxidases.

Acknowledgements

We thank Maria Chiara Silvestrini for critical reading of the manuscript, Michel Denis, Wilfred Hagen, Michael T. Wilson and Walter Zumft for very stimulating discussions, our students Flavia Nicoletti and Alessandro Giuffre' for their everlasting questions and Emilio D'Itri for skilful biochemical preparations. Work partially supported by MURST (40% 'Liveprotein') and by a CEE grant no. SC1-CT91-0698 (CAESAR project).

References

[1] M. Brunori, G. Antonini, F. Malatesta, P. Sarti and M.T. Wilson, Adv. Inorg. Biochem., 7 (1987) 93.
[2] J. Inorg. Biochem., 23 (1985); Ann. N.Y. Acad. Sci., 550 (1988). These two issues are accounts of the proceedings of meetings on cytochrome oxidase held in Rome between October 3–6, 1984 and June 20–21, 1988.
[3] M.K.F. Wikström, K. Krab and M. Saraste, Cytochrome Oxidase. A synthesis, Academic Press, New York, 1981.
[4] M.K.F. Wikström, Nature (London), 266 (1977) 271.
[5] P. Mitchell, Chemiosmotic Coupling in Oxidative and Photosynthetic Phosporylation, Glynn Research, Bodmin, 1966.
[6] T. Yonetani, J. Biol. Chem., 235 (1960) 845.
[7] T. Yonetani, J. Biol. Chem., 236 (1961) 1680.
[8] N.C. Robinson and R.A. Capaldi, Biochemistry, 16 (1977) 375.
[9] M. Saraste, T. Penttilä, and M. Wikström, Eur. J. Biochem., 115 (1981) 261.
[10] M. Tihova, B. Tattrie, P. Nicholls, Biochem. J., 292 (1993) 933.
[11] M.T. Wilson, W. Lalla-Maharajh, V.M. Darley-Usmar, J. Bonaventura, C. Bonaventura and M. Brunori, J. Biol. Chem., 255 (1980) 2712.
[12] V.M. Darley-Usmar, N. Alizai, A.I. Al-Ayash, J.D. Jones, A. Sharpe and M.T. Wilson, Comp. Biochem. Physiol., 68B (1981) 445.
[13] M. Wikström, K. Krab and M. Saraste, Ann. Rev. Biochem., 50 (1981) 623.
[14] R. Bisson, B. Jacobs and R.A. Capaldi, Biochemistry, 19 (1980) 4173.
[15] G. Georgevich, V.M. Darley-Usmar, F. Malatesta and R.A. Capaldi, Biochemistry, 22 (1983) 1317.
[16] F. Malatesta, G. Antonini, P. Sarti and M. Brunori, Biochem. J., 234 (1986) 569.
[17] M. Brunori, G. Antonini, F. Malatesta, P. Sarti and M.T. Wilson, Eur. J. Biochem., 169 (1987) 1.
[18] G. Antonini, M. Brunori, F. Malatesta, P. Sarti and M.T. Wilson, J. Biol. Chem., 262 (1987) 10077.
[19] M.T. Wilson, M. Brunori, P. Sarti, G. Antonini and F. Malatesta, Chem. Scripta, 28A (1988) 57.
[20] G. Buse, G.C.M. Steffens and L. Meinecke, in E. Quagliarello and F. Palmieri (Editors), Structure and Function of Membrane Proteins, Amsterdam, Elsevier, 1983, p. 131.
[21] B. Kadenbach, L. Kuhn-Nentwig and U. Büge, Curr. Top. Bioenerg., 15 (1987) 113.
[22] R. Poole, in C. Anthony (Editor), Bacterial Energy Transduction, Academic Press, New York, 1988, p. 231.
[23] J.A. Fee, T. Yoshida, K.K. Surerus and M.W. Mather, J. Bioen. and Biomem., 25 (1993) 103.
[24] M. Saraste, Quart. Rev. Biophys., 23 (1990) 331.
[25] R. Henderson, R.A. Capaldi and J.S. Leigh, J. Mol. Biol., 122 (1977) 631.
[26] T.G. Frey, S.H.P. Chan and G. Schatz, J. Biol. Chem., 253 (1978) 4389.
[27] S.D. Fuller, R.A. Capaldi and R. Henderson, J. Mol. Biol., 134 (1979) 305.
[28] J.M. Valpuesta, R. Henderson and T.G. Frey, J. Mol. Biol., 214 (1990) 237.
[29] J.F. Deatherage, R. Henderson and R.A. Capaldi, J. Mol. Biol., 158 (1982) 487.
[30] G.C.M. Steffens, R. Biewald and G. Buse, Eur. J. Biochem., 164 (1987) 295.
[31] O. Warburg, Biochem. Z., 152 (1924) 479.
[32] C.R. Hartzell and H. Beinert, Biochim. Biophys. Acta, 368 (1974) 318.
[33] R.F. Van Gelder and H. Beinert, Biochim. Biophys. Acta, 189 (1969) 1.
[34] T. Yonetani, Biochim. Biophys. Res. Commun., 3 (1960) 549.
[35] R. Aasa, S.P.J. Albracht, K.E. Falk, B. Lanne and T. Vänngård, Biochim. Biophys. Acta, 422 (1976) 260.
[36] O. Einarsdottir and W.S. Caughey, Biochim. Biophys. Res. Commun., 124 (1984) 836.
[37] O. Einarsdottir and W.S. Caughey, Biochim. Biophys. Res. Commun., 129 (1984) 840.

[38] D. Keilin and E.F. Hartree, Proc. R. Soc. London, Ser. B, 127 (1939) 167.
[39] S. Horie and M. Morrison, J. Biol. Chem., 238 (1963) 2859.
[40] W.A. Vanneste, Biochemistry, 5 (1966) 838.
[41] D.F. Blair, D.F. Bocian, G.T. Babcock and S.I. Chan, Biochemistry, 21 (1982) 6928.
[42] C.R. Hartzell, R.E. Hansen and H. Beinert, Proc. Natl. Acad. Sci. USA, 70 (1973) 2477.
[43] D.E. Griffiths and D.C. Wharton, J. Biol. Chem., 236 (1961) 1857.
[44] D.C. Wharton and A. Tzagoloff, J. Biol. Chem., 239 (1964) 2036.
[45] H. Beinert, C.R. Hartzell, W.H. Orme-Johnson, in B. Chance, T. Yonetani and A.S. Mildran (Editors), Probes of Structure and Function of Macromolecules and Membranes, Vol. 2, Academic Press, New York, pp. 575–592.
[46] P.M.H. Kroneck, M.A. Antholine, J. Riester and W.G. Zumft, FEBS Lett., 242 (1988) 70.
[47] H. Beinert in J. Peisach, P. Alisen and W.E. Blumberg (Editors), The Biochemistry of Copper, Academic Press, New York 1966.
[48] R.A. Malkin and B.G. Malmström, Adv. Enzymol., 33 (1970) 177.
[49] J. Peisach and W.E. Blumberg, Arch. Biochem. Biophys., 165 (1974) 691.
[50] G.C.M. Steffens and G. Buse, Hoppe Seyler's Z. Physiol. Chem., 360 (1979) 5613.
[51] S.I. Chan, D.F. Bocian, G.W. Brudwig, R.H. Morse and T.H. Stevens, in T.E. King, Y. Orii, B. Chance and K. Okunuki (Editors), Cytochrome Oxidase, Elsevier, Amsterdam, 1979, p. 177.
[52] T.H. Stevens, C.T. Martin, H. Wang, G.W. Brudvig, C.P. Scholes and S.I. Chan, J. Biol. Chem., 257 (1982) 12106.
[53] C.T. Martin, C.P. Scholes and S.I. Chan, J. Biol. Chem., 263 (1988) 8420.
[54] V.W. Hu, S.I. Chan and G.S. Brown, FEBS Lett., 84 (1977) 287.
[55] R.A. Scott, S.P. Cramer, R.W. Shaw, H. Beinert and H.B. Gray, Proc. Natl. Acad. Sci. USA, 78 (1981) 664.
[56] C. Greenwood, B.C. Hill, D. Barber, D.G. Englinton and A.J. Thomson, Biochem. J., 215 (1983) 303.
[57] B.M. Hoffman, J.E. Roberts, M. Swansson, S.H. Speck and E. Margoliash, Proc. Natl. Acad. Sci. USA, 77 (1980) 1452.
[58] L. Calabrese, M. Carbonaro and G. Musci, J. Biol. Chem., 263 (1988) 6480.
[59] D.M. Dooley, R.S. Moog and W.G. Zumft, J. Am. Chem. Soc., 109 (1987) 6730.
[60] R.A. Scott, W.G. Zumft, C.L. Coyle and D.M.Dooley, Proc. Natl. Acad Sci. USA, 86 (1989) 4082.
[61] S. Takahashi, T. Ogura, K. Itoh-Shinzawa, S. Yoshikawa and T. Kitagawa J. Am. Chem. Soc., 113 (1991) 9400.
[62] B.G. Malmström and R. Aasa, FEBS, 325 (1993) 49.
[63] M. Kelly, P. Lappalainen, G. Talbo, T. Haltia, J. van der Oost and M. Saraste, J. Biol. Chem., 268 (1993) 16781.
[64] P. Lappalainen, R. Aasa, B.G. Malmström and M. Saraste, J. Biol. Chem., 268 (1993) 26416.
[65] G.T. Babcock, P.M. Callahan, M.R. Ondrias and I. Salmeen, Biochemistry, 20 (1981) 959.
[66] G.T. Babcock, J. Van Steelan, G. Palmer, L.E. Vickery, I. Salmeen, in T.E. King, Y. Orii, B. Chance and K. Okunuki (Editors), Cytochrome Oxidase, Elsevier, Amsterdam, 1979, p. 105.
[67] K. Carter and G. Palmer, J. Biol. Chem., 257 (1982) 13507.
[68] D.G. Eglinton, M.K. Johnson, A.J. Thomson, P.E. Gooding and C. Greenwood, Biochem. J., 191 (1980) 319.
[69] K.E. Falk, T. Vänngård and J. Angstrom, FEBS Lett., 75 (1977) 23.
[70] M.F. Tweedle, L.J. Wilson, L. Garcia-Inigues, G.T. Babcock and G. Palmer, J. Biol. Chem., 253 (1978) 8065.
[71] A.J. Thomson, T. Brittain, C. Greenwood and J.P. Springall, Biochem. J., 165 (1977) 327.
[72] C.H.A. Seiter and S.G. Angelos, Proc. Natl. Acad. Sci. USA, 77 (1980) 1806.
[73] P. Nicholls and B.A. Chanady, Biochim. Biophys. Acta, 634 (1981) 256.
[74] D. Bickar, C. Bonaventura and J. Bonaventura, J. Biol. Chem., 259 (1984) 10777.
[75] D.F. Blair, S.N. Witt and S.I. Chan, J. Am. Chem. Soc., 107 (1985) 7389.
[76] T.A. Kent, L.J. Young, G. Palmer, J.A. Fee and E. Munck, J. Biol. Chem., 258 (1983) 8543.
[77] T.H. Stevens, G.W. Brudvig, D.F. Bocian and S.I. Chan, Proc. Natl. Acad. Sci. USA, 76 (1979) 3320.
[78] L. Powers, B. Chance, Y. Ching and P. Angiolillo, Biophys. J., 34 (1981) 465.
[79] R.A. Scott, P.M. Li and S.I. Chan, Ann. N.Y. Acad. Sci., 550 (1988) 53.
[80] B. Reinhammar, R. Malkin, P. Jensen, B. Karlsson, L. Andreasson, R. Aasa, T. Vänngård and B.G. Malmström, J. Biol. Chem., 255 (1980) 5000.
[81] B. Karlsson, R. Aasa, T. Vänngård and B.G. Malmström, FEBS Lett., 131 (1981) 186.
[82] S.N. Witt, D.F. Blair and S.I. Chan, J. Biol. Chem., 261 (1986) 8104.
[83] M.F.T. Blokzijl Homan and B.F. Van Gelder, Biochim. Biophys. Acta, 234 (1971) 493.
[84] T.H. Stevens, D.F. Bocian and S.I. Chan, FEBS Lett., 97 (1979) 314.
[85] T.H. Stevens and S.I. Chan, J. Biol. Chem., 256 (1981) 1069.
[86] J. Cline, B. Reinhammar, P. Jensen, R. Venters and B.M. Hoffman, J. Biol. Chem., 258 (1983) 5124.
[87] B.V. Shaw, R.E. Hansen and H. Beinert, J. Biol. Chem., 253 (1978) 6637.
[88] E. Antonini, M. Brunori, A. Colosimo, C. Greenwood and M.T. Wilson, Proc. Natl. Acad. Sci. USA, 74 (1977) 3128.
[89] B.V. Shaw, R.E. Hansen and H. Beinert, Biochim. Biophys. Acta, 548 (1979) 386.
[90] A. Naqui, L. Powers, M. Lundeen and B. Chance, Biophys. J., 51 (1987) 312.
[91] L. Holm, M. Saraste and M.K.F. Wikström, EMBO J., 6 (1987) 2819.

[92] R. Bisson, in G. Milaaazzo and M. Blank (Editors), Bioelectrochemistry III: Charge Separation across Biomembranes, Plenum Press, New York, 1988, p. 125.
[93] T. Haltia, A. Puustinen and M. Finel, Eur. J. Biochem., 172 (1988) 543.
[94] Y. Anraku and R.B. Gennis, Trends Biochem. Sci., 12 (1987) 262.
[95] V. Chepuri, L. Lemieux, D.C.T. Au and R.B. Gennis, J. Biol. Chem., 265 (1990) 12978.
[96] A. Puustinen, M. Finel, T. Haltia, R.B. Gennis and M. Wikström, Biochemistry, 30 (1991) 3936.
[97] G.T. Babcock and M. Wikström, Nature (London), 356 (1992) 301.
[98] J. van der Oost, P. Lappalainen, A. Musacchio, A. Wayne, L. Lemieux, J. Rumbley, R.B. Gennis, R. Aasa, T. Pascher, B.G. Malmström and M. Saraste, EMBO J., 11 (1992) 3209.
[99] J.P.Shapleigh, J.P. Hosler, M.M.J. Tecklenburg, T. Kim, G.T. Babcock, R.G. Gennis and S. Ferguson-Miller, Proc. Natl. Acad. Sci. USA, 89 (1992) 4786.
[100] J.P. Hosler, S. Ferguson-Miller, M.W. Calhoun, J.W. Thomas, J. Hill, L. Lemieux, J. Ma, C. Georgiou, J. Fetter, J. Shapleigh, M.M.J. Tecklenburg, G.T. Babcock and R.B. Gennis, J. Bioenerg. Biomem., 25 (1993) 121.
[101] M. Brunori, C. Colosimo, G. Rainoni, M.T. Wilson and E. Antonini, J. Biol. Chem., 254 (1979) 10769.
[102] G. Antonini, M. Brunori, A. Colosimo, F. Malatesta and P. Sarti, J. Inorg. Biochem., 23 (1985) 289.
[103] U. Brandt, H. Schägger and G. Von Jagow, Eur. J. Biochem., 182 (1989) 705.
[104] P. Nicholls, K.J.H. Van Buuren and B.F. Van Gelder, Biochim. Biophys. Acta, 275 (1972) 279.
[105] G.M. Baker, M. Noguchi and G. Palmer, J. Biol. Chem., 262 (1987) 595.
[106] P. Sarti, G. Antonini, F. Malatesta and M. Brunori, Biochem. J., 284 (1992) 123.
[107] P. Sarti, A. Colosimo, M. Brunori, M.T. Wilson and E. Antonini, Biochem. J., 209 (1983) 81.
[108] C. Bonaventura, J. Bonaventura, M. Brunori and M.T. Wilson, FEBS Lett., 85 (1978) 30.
[109] W.H. Woodruff, J. Bioenerg. Biomem., 25 (1993) 177.
[110] M. Brunori and M.T. Wilson, Trends Biochem. Sci., 7 (1982) 295.
[111] A.J. Moody, U. Brandt and P.R. Rich, FEBS Lett., 293 (1991) 101.
[112] M.G. Jones, D. Bickar, M.T. Wilson, M. Brunori, A. Colosimo andP. Sarti, Biochem. J., 220 (1984) 57.
[113] P. Jensen, M.T. Wilson, R. Aasa and B.G. Malmström, Biochem. J., 224 (1984) 829.
[114] H.B. Gray and B.G. Malmström, Biochemistry, 28 (1989) 7499.
[115] M.T. Wilson, G. Antonini, F. Malatesta, P. Sarti and M. Brunori, J. Biol. Chem., 269 (1994) 24114.
[116] Q.H. Gibson, C. Greenwood, D.C. Wharton and G. Palmer, J. Biol. Chem., 240 (1965) 888.
[117] L.E. Andreasson, B.G. Malmström, C. Stromberg and T. Vänngård, FEBS Lett., 28 (1972) 297.
[118] M.T. Wilson, C. Greenwood, M. Brunori and E. Antonini, Biochem. J., 147 (1975) 145.
[119] T.M. Antalis and G. Palmer, J. Biol. Chem., 257 (1982) 6194.
[120] K.J.H. Van Buuren, B.F. Van Gelder, J. Wilting and R. Braams, Biochim. Biophys. Acta, 333 (1974) 421.
[121] L.G. Petersen and L.E. Andreasson, FEBS Lett., 66 (1976) 52.
[122] C. Greenwood, T. Brittain, M.T. Wilson and M. Brunori, Biochem. J., 157 (1976) 591.
[123] E.C.I. Veerman, J.W. Van Leeuwen, K.J.H. Van Buuren and B.F. Van Gelder, Biochim. Biophys. Acta, 680 (1982) 134.
[124] G.D. Jones, M.G. Jones, M.T. Wilson, M. Brunori, A. Colosimo and P. Sarti, Biochem. J., 209 (1983) 175.
[125] R.A. Scott and H.B. Gray, J. Am. Chem. Soc., 102 (1980) 3219.
[126] P. Sarti, F. Malatesta, G. Antonini, B. Vallone and M. Brunori, J. Biol. Chem., 265 (1990) 5554.
[127] F. Malatesta, G. Antonini, P. Sarti, B. Vallone and M. Brunori, Biol. Metals, 3 (1990) 118.
[128] E. Margoliash and H.R. Bosshard, Trends Biochem. Sci., 8 (1983) 316.
[129] C.H.A. Seiter, R. Margalit and R.A. Berreault, Biochem. Biophys. Res. Commun., 86 (1979) 473.
[130] F. Millett, V.M. Darley-Usmar and R.A. Capaldi, Biochemistry, 21 (1982) 3857.
[131] F. Millett, C. de Jong, L. Paulson and R.A. Capaldi, Biochemistry, 22 (1983) 546.
[132] R. Bisson and C. Montecucco, FEBS Lett., 150 (1982) 49.
[133] R. Bisson, A. Azzi, H. Gutweniger, R. Colonna, C. Montecucco and A. Zanotti, J. Biol. Chem., 253 (1978) 1874.
[134] W. Birchmeier, C.E. Kohler and G. Schatz, Proc. Natl. Acad. Sci. USA, 73 (1976) 4334.
[135] S.D. Fuller, V.M. Darley-Usmar and R.A. Capaldi, Biochemistry, 20 (1981) 7046.
[136] F. Malatesta and R.A. Capaldi, Biochem. Biophys. Res. Commun., 109 (1982) 1180.
[137] R.A. Capaldi, F. Malatesta and V.M. Darley-Usmar, Biochim. Biophys. Acta, 726 (1983) 135.
[138] J.T. Hazzard, S. Rong and G. Tollin, Biochemistry, 30 (1991) 213.
[139] J. Gelles and S.I. Chan, Biochemistry, 24 (1985) 3963.
[140] K. Kobayashi, H. Une and K. Hayashi, J. Biol. Chem., 264 (1989) 7976.
[141] T. Nilsson, Proc. Natl. Acad. Sci. USA, 89 (1992) 6497.
[142] Z. Li, R.W. Larsen, L. Pan and S.I. Chan, J. Biol. Chem., 266 (1991) 22858.
[143] L. Pan, J.T. Hazzard, J. Lin, G. Tollin and S.I. Chan, J. Am. Chem. Soc., 113 (1991) 5908.
[144] G. Buse, L. Meinecke and B. Bruch, J. Inorg. Biochem., 23 (1985) 149.
[145] T. Alleyne, M.T. Wilson, G. Antonini, F. Malatesta, B.

Vallone, P. Sarti and M. Brunori, Biochem. J., 287 (1992) 951.
[146] B. Hill, J. Biol. Chem., 266 (1991) 2219.
[147] C.R. Hartzell and H. Beinert, Biochim. Biophys. Acta, 423 (1976) 323.
[148] N. Schroedl and C.R. Hartzell, Biochemistry, 16 (1977) 4961.
[149] J.S. Lindsay, C.S. Owen and D.F. Wilson, Arch. Biochem. Biophys., 169 (1975) 492.
[150] R.P.Carithers and G. Palmer, J. Biol. Chem., 256 (1981) 7967.
[151] W.R.Ellis, H. Wang, D.F. Blair, H.B. Gray and S.I. Chan, Biochemistry, 25 (1986) 161.
[152] H. Wang, D.F. Blair, W.R, Ellis, H.B. Gray and S.I. Chan, Biochemistry, 25 (1986) 167.
[153] D.F. Blair, W.R. Ellis, H. Wang, H.B. Gray and S.I. Chan, J. Biol. Chem., 261 (1986) 11524.
[154] J.E. Morgan, P.M. Li, D. Jang, M.A. El-Sayed and S.I. Chan, Biochemistry, 28 (1989) 6975.
[155] P. Nicholls and L.C. Peterson, Biochim. Biophys. Acta, 357 (1974) 462.
[156] M. Wikström, H.J. Harmon, W.J. Ingledew and B. Chance, FEBS Lett., 65 (1976) 259.
[157] B.G. Malmström, Chem. Rev., 90 (1990) 1247.
[158] G. Goodman, J. Biol. Chem., 259 (1984) 15094.
[159] D. Walz, Biochim. Biophys. Acta, 505 (1979) 279.
[160] B. Lanne and T. Vänngård, Biochim. Biophys. Acta, 501 (1978) 449.
[161] M. Coletta, T. Catarino, J. LeGall and A.V. Xavier, Eur. J. Biochem., 202 (1991) 1101.
[162] M. Wikström, Chem. Scripta, 27B (1987) 53.
[163] M. Wikström, Chem. Scripta, 28A (1988) 71.
[164] M. Wikström, Proc. Natl. Acad. Sci. USA, 78 (1981) 4051.
[165] D. Bickar, J.F. Turrens and A.L. Lehninger, J. Biol. Chem., 261 (1986) 14461.
[166] R. Boelens, R. Wever and B.F. Van Gelder, Biochim. Biophys. Acta, 682 (1982) 264.
[167] P. Brzezinski and B.G. Malmström, Biochim. Biophys. Acta, 894 (1987) 29.
[168] W.H. Woodruff, O. Einarsdottir, R.B. Dyer, K.A. Bagley, G. Palmer, S.J. Atherton, R.A. Goldbeck, T.D. Dawes and D.S. Kliger, Proc. Natl. Acad. Sci. USA, 88 (1991) 2588.
[169] P. Sarti, G. Antonini, F. Malatesta, B. Vallone and M. Brunori, Ann. N.Y. Acad. Sci., 550 (1988) 161.
[170] F.Malatesta, P. Sarti, G. Antonini, B. Vallone and M. Brunori, Proc. Natl. Acad. Sci. USA, 87 (1990) 7410.
[171] E. Antonini, M. Brunori, C. Greenwood and B.G. Malmström, Nature (London), 228 (1970) 936.
[172] S. Ferguson-Miller, D.L. Brautigan and E. Margoliash, J. Biol. Chem., 251 (1976) 1104.
[173] E.A.E. Garber and E. Margoliash, Biochim. Biophys. Acta, 1015 (1990) 279.
[174] R.B. Dyer, O. Einarsdottir, P.M. Killough, J.J. Lopez-Garriga and W.H. Woodruff, J. Am. Chem. Soc., 111 (1989) 7657.
[175] R.A. Marcus and N. Sutin, Biochim. Biophys. Acta, 811 (1985) 265.
[176] H.B. Gray and B.G. Malmström, Biochemistry, 28 (1989) 7499.
[177] Q.H. Gibson and C. Greenwood, Biochem. J., 86 (1960) 51.
[178] Q.H. Gibson and C. Greenwood, J. Biol. Chem., 240 (1965) 2694.
[179] C. Greenwood and Q.H. Gibson, J. Biol. Chem., 242 (1967) 1782.
[180] J.K.V. Reichardt and Q.H. Gibson, J. Biol. Chem., 257 (1982) 9268.
[181] M. Brunori and Q.H. Gibson, EMBO J., 2 (1983) 2025.
[182] B.C. Hill and C. Greenwood, Biochem. J., 218 (1984) 913.
[183] Y. Orii, J. Biol. Chem., 259 (1984) 7187.
[184] Q.H. Gibson and C. Greenwood, Biochem. J., 86 (1963) 541.
[185] B. Chance, C. Saronio and J.S. Leigh, Proc. Natl. Acad. Sci. USA, 72 (1975) 1635.
[186] B. Chance, C. Saronio and J.S. Leigh, J. Biol. Chem., 250 (1975) 9226.
[187] G.M. Clore, L.E. Andreasson, B. Karlsson, R. Aasa and B.G. Malmström, Biochem. J., 185 (1980) 139.
[188] G.M. Clore, L.E. Andreasson, B. Karlsson, R. Aasa and B.G. Malmström, Biochem. J., 185 (1980) 155.
[189] S. Han, Y. Ching and D.L. Rousseau, Proc. Natl. Acad. Sci. USA, 87 (1990) 2491.
[190] S. Han, Y. Ching and D.L. Rousseau, Proc. Natl. Acad. Sci. USA, 87 (1990) 8408.
[191] S. Han, Y. Ching and D.L. Rousseau, J. Am. Chem. Soc., 111 (1990) 9446.
[192] M. Oliveberg, S. Hallen and T. Nilsson, Biochemistry, 30 (1991) 436.
[193] S. Hallen and T. Nilsson, Biochemistry, 31 (1992) 11853.
[194] S. Han, Y. Ching and D.L. Rousseau, Nature (London), 348 (1990) 88.
[195] C. Varotsis Y. Zhang, E.H. Appelman and G.T. Babcock, Proc. Natl. Acad. Sci. USA, 90 (1993) 237.
[196] M. Oliveberg, P. Brzezinski and B.G. Malmström, Biochim. Biophys. Acta, 977 (1989) 322.
[197] M. Wikström, Nature (London), 338 (1989) 776.
[198] S.I. Chan and P.M. Li, Biochemistry, 29 (1990) 1.
[199] R.S. Blackmore, C. Greenwood and Q.H. Gibson, J. Biol. Chem., 266 (1991) 19245.
[200] M. Oliveberg and B.G. Malmström, Biochemistry, 31 (1992) 3560.
[201] M. Brunori, G. Antonini, F. Malatesta, P. Sarti and M.T. Wilson, FEBS Lett., 314 (1992) 191.
[202] J.E. Morgan and M. Wikström, Biochemistry, 30 (1991) 948.
[203] S.I. Chan, S.N. Witt and D.F. Blair, Chem. Scripta, 28A (1988) 51.
[204] T.V. Vygodina and A.A. Kostantinov, Ann. N.Y. Acad. Sci., 550 (1988) 124.
[205] F. Malatesta, G. Antonini, P. Sarti, B. Vallone and M. Brunori, Ann. N.Y. Acad. Sci., 550 (1988) 269.
[206] M.I. Verkhovsky, J.E. Morgan and M. Wikström, Biochemistry, 31 (1992) 11860.
[207] H. Michel, O. Epp and J. Deisenhofer, J. Mol. Biol., 5 (1986) 2445.

[208] A. Messerschmidt, A. Rossi, R. Landenstein, R. Huber, M. Bolognesi, M. Gatti, A. Marchesini, R. Petruzzelli and A. Finazzi-Agró, J. Mol. Biol., 206 (1989) 513.
[209] K. Krab and M.K.F. Wikström, Biochim. Biophys. Acta, 504 (1978) 200.
[210] R.P. Casey, J.B. Chappell and A. Azzi, Biochem. J., 182 (1979) 149.
[211] J.T. Coin and P.C. Hinkle, in C.P. lee, G. Schatz and L. Ernster (Editors), Membrane Bioenergetics, Addison-Wesley, Reading, 1979, p. 405.
[212] E. Sigel and E. Carafoli, Eur. J. Biochem., 111 (1980) 299.
[213] P. Sarti, M.G. Jones, A. Antonini, F. Malatesta, A. Colosimo, M.T. Wilson and M. Brunori, Proc. Natl. Acad. Sci. USA, 82 (1985) 4876.
[214] P.C. Hinkle, J.J. Kim and E. Racker, J. Biol. Chem., 247 (1972) 1338.
[215] E. Racker, Meth. Enzymol., 55 (1979) 699.
[216] R.P. Casey, Biochim. Biophys. Acta, 768 (1984) 319.
[217] V.M. Darley-Usmar, R.A. Capaldi, S. Takamiya, F. Millett, M.T. Wilson, F. Malatesta and P. Sarti, in V.M. Darley-Usmar, D. Rickwood and M.T. Wilson (Editors), Mitochondria: A Practical Approach, IRL Press, Oxford, Chapter 5, p. 113.
[218] Y. Kagawa and E. Racker, J. Biol. Chem., 241 (1966) 2467.
[219] M. Müller and A. Azzi, J. Bioenerg. Biomem., 17 (1985) 385.
[220] P. Sarti, G. Antonini, F. Malatesta, B. Vallone, S. Villaschi, M. Brunori, R.C. Hider and K. Hamed, Biochem. J., 257 (1989) 783.
[221] M. Finel and M. Wikström, Biochim. Biophys. Acta, 851 (1986) 99.
[222] P. Sarti, F. Malatesta, G. Antonini, A. Colosimo and M. Brunori, Biochim. Biophys. Acta, 809 (1985) 39.
[223] L. Gregory and S. Ferguson-Miller, Biochemistry, 28 (1989) 2655.
[224] N. Capitanio, E. De Nitto, G. Villani, G. Capitanio and S. Papa, Biochemistry, 29 (1990) 2939.
[225] P. Sarti, F. Malatesta, G. Antonini, B. Vallone and M. Brunori, J. Biol. Chem., 265 (1990) 5554.
[226] G. Antonini, F. Malatesta, P. Sarti and M. Brunori, J. Biol. Chem., 266 (1991) 13193.
[227] C.E. Cooper, Biochim. Biophys. Acta, 1017 (1990) 187.
[228] J.M. Wrigglesworth, C.E. Cooper, M.A. Sharpe and P. Nicholls, Biochem. J., 270 (1990) 109.
[229] F. Malatesta, G. Antonini, P. Sarti and M. Brunori, Biochem. J., 248 (1987) 161.
[230] G. Antonini, F. Malatesta, P. Sarti and M. Brunori, Proc. Natl. Acad. Sci. USA, 90 (1993) 5949.
[231] B. Maison-Peteri and B.G. Malmström, Biochemistry, 28 (1989) 3156.
[232] M. Brunori, P. Sarti, A. Colosimo, G. Antonini, F. Malatesta, M.G. Jones and M.T. Wilson, EMBO J., 4 (1985) 2365.
[233] J.M. Wrigglesworth, J. Inorg. Biochem., 23 (1985) 311.
[234] K. Krab and M. Wikström, Biochim. Biophys. Acta, 548 (1979) 1.
[235] M. Brunori, P. Sarti, G. Antonini and F. Malatesta, Bioelectrochem. Bioenerg., 16 (1986) 159.
[236] E.R. Henry and J. Hofrichter, Meth. Enzymol., 210 (1992) 129.
[237] J. Wyman, Accad. Naz. Lincei, Serie VIII, 64 (1978) 409.
[238] M. Brunori, M. Coletta, B. Giardina and J. Wyman, Proc. Natl. Acad. Sci. USA, 75 (1978) 4310.
[239] J.F. Naggle and S. Tristram-Nagle, J. Mem. Biol., 74 (1983) 1.
[240] G.T. Babcock and P.M. Callahan, Biochemistry, 22 (1983) 2314.
[241] T. Nilsson, J. Gelles, P.M. Li and S.I. Chan, Biochemistry, 27 (1988) 296.
[242] J. Gelles, D.F. Blair and S.I. Chan, Biochim. Biophys. Acta, 853 (1986) 205.
[243] P.Nicholls, Biochem. J., 228 (1992) 1070.
[244] O. Einasdottir, P.M. Killough, J.A. Fee and W.H. Woodruff, J. Biol. Chem., 264 (1989) 2405.
[245] C.C. Moser, J.M. Keske, K. Warncke, R.S. Farid and P.L. Dutton, Nature (London), 355 (1992) 796.
[246] M. Brunori, G. Antonini, A. Giuffre, F. Malatesta, F. Nicoletti, P. Sarti and M.T. Wilson, FEBS Lett., 350 (1994) 164.
[247] D. Rousseau, Y. Ching and J. Wang, J. Bioenerg. Biomem., 25 (1993) 165.